TWO PHASE, GAS-LIQUID FLOW THROUGH A VERTICAL CHANNEL

by

Benoît Pouliquen

A thesis submitted to the Faculty of Graduate Studies and Research in partial fulfillment of the requirements for the degree of Master of Engineering

Department of Mining and
Metallurgical Engineering,
McGill University,
Montreal,
Canada.

,A KARINE

" -Je connais une planète où il y a un Monsieur cramoisi. Il n'a jamais respiré une fleur. Il n'a jamais regardé une étoile. Il n'a jamais aimé personne. Il n'a jamais rien fait d'autre que des additions. Et toute la journée il répète comme toi :"Je suis un homme sérieux! Je suis un homme sérieux!" et ça le fait gonfler d'orgueil.

-Il y a des millions d'années que les fleurs fabriquent des épines. Il y a des millions d'années que les moutons mangent quand même les fleurs. Et ce n'est pas sérieux de chercher à comprendre pourquoi elles se donnent tant de mal pour se fabriquer des épines qui ne servent jamais à rien? Ce n'est pas important la guerre des moutons et des fleurs? Ce n'est pas plus sérieux et plus important que les additions d'un gros Monsieur tout rouge?"

Antoine de Saint-Exupery

Le Petit Prince

ABSTRACT

A new technique to enhance vacuum refining kinetics of molten metals is under development. In this process known as "Lift-Spray Vacuum Refining", gas is injected at the bottom of a vertical tube immersed in the liquid metal. The molten metal is lifted from a point beneath the bath surface to a point above the bath surface where it is dispersed in the vacuum by the action of the gas bubbles exploding into the vacuum. Experiments were carried out on an aqueous model in order to understand the physical characteristics of the two-phase flow phenomena under vacuum.

Cold model experiments have shown that:

- low pressures favour churn-turbulent bubbly flows
- a maximum potential lift L^* exists for any set of conditions
- when the size of the lifter is less than L^*, overflow occurs.

A theoretical model has been developed to describe the two-phase flow phenomena in terms of Lifter Diameter, Lifter Height, Nozzle Submergence and volumetric gas flow rate. This model predicts the potential lift in a lifting tube as well as the overflow rate in a lift-overflow system. Both of these predictions are confirmed quantitatively by the experiments and data previously obtained in similar processes.

The model which is thought to be applicable to gas injection into liquid metals shows that the important parameter is the volumetric flow rate of gas. Consequently, for a given molar flow rate, the application of vacuum enhances lift and overflow rates.

RESUME

Une technique nouvelle ayant pour but d'améliorer la cinétique d'affinage sous vide des métaux en fusion est actuellement dans sa phase de développement. Dans ce procédé, connu sous le nom d'affinage sous vide "Lift-Spray", du gaz est injecté à la base d'un tube vertical immergé dans le métal liquide. Le métal en fusion est amené d'un point situé sous la surface du bain jusqu'à un point au dessus de cette surface, où il est dispersé en fines goutelettes par l'action des bulles gazeuses explosant dans le vide. Les expériences conduites sur un modèle aqueux ont eu pour but de comprendre les caractéristiques physiques de l'écoulement diphasique.

Les expériences ont démontré que:

- les basses pressions favorisent un régime d'écoulement turbulent
- Il existe, pour le mélange dans le tube, un niveau potentiel maximum, L^*, quelles que soient les conditions
- quand la taille du tube est inférieure à L^*, le liquide déborde.

Un modèle théorique a été développé pou décrire le phénomène d'écoulement diphasique en fonction du diamètre du tube, de sa hauteur, de la profondeur de l'injecteur et du

débit volumique du gaz. Ce modèle prédit le niveau potentiel atteint par le mélange de même que le débit du liquide lorsque celui-ci déborde. Ces deux prédictions sont confirmées quantitativement par les expériences et les données obtenues sur des procédés similaires.

Le modèle, applicable au métal liquide, montre que le paramètre important est le débit volumique du gaz. En conséquence, pour un débit molaire donné, les basses pressions augmentent le niveau potentiel dans la colonne ainsi que le débit du liquide.

ACKNOWLEDGEMENTS

I extend my deepest thanks to Professor Ralph Harris for his ideas, enthusiasm and sincerity in his approach to my studies.

I also wish to thank Steve Dawson for his help with the experimental work.

All other staff, both technical and academic, of the Department of Metallurgical Engineering, McGill University, receive my appreciation for making the time I spent with them most enjoyable.

Je tiens tout spécialement à remercier ceux qui m'ont entouré pendant cette année et sans lesquels ce travail ne saurait être ce qu'il est. Ils sauront se reconnaître.

Enfin, j'adresse mes remerciements à Pascal Ernstberger qui, un matin du mois d'août, m'a aidé dans mes premières expériences et a su me donner confiance pour mener ce travail à bien.

TABLE OF CONTENTS

LIST OF FIGURES

LIST OF TABLES

CHAPTER ONE

INTRODUCTION

1.1 General

Two-Phase flow, as the name implies, refers to the general case where a mixture of two components, sometimes but not necessarily having different phases, move fluidly. Phases can be either gas, liquid, or solid. Sometimes, phases consist of the same chemical substance, for example, steam-water flows while in other examples the components may be different, e.g. air-water flows. The two phases may be moving colinearly or countercurrently and the mathematics which describe either two-component or two-phase flows are identical.

In industry, many processes in chemical engineering, nuclear science, metallurgy, etc., are concerned with multiphase flows. The phenomena are not yet well understood because of the complexity of their analysis, and improvements in the understanding will occur in the future.

In particular, the use of gas injection in liquid metals for physical and chemical purposes is under constant development. Systems have been developed by the Metallurgical Industry for use either under ambient pressures or under vacuum. This work was undertaken to quantify the effect of low pressure on two-phase flow phenomena in the

particular case where gas in injected into a liquid with the gas-liquid flow constrained in a vertical tube.

1.2. The Thesis

This thesis examines two-phase flow phenomena in a gas-lift pump. The principle of such systems is to inject a gas into a liquid at the bottom of a so-called lifting tube so that the buoyancy of the gas bubbles drives the liquid above the free surface of the bath. From the top of the lifter, if it is so designed, the liquid can fall back into the bath.

The second chapter of the thesis summarizes previous two-phase flow studies and experimental measurements of circulation rates are described in Chapter Three. Photographic studies of two-phase flow phenomena are shown in Chapter Four. Chapter Five examines the experimental values of the circulation rates. A new theoretical model of gas-lift pumps is developed in Chapter Six and a comparison between the predicted theoretical flow rates is made in Chapter Seven. Finally, future work is suggested and conclusions are drawn in Chapter Eight.

CHAPTER TWO

ONE DIMENSIONAL TWO-PHASE FLOW: GENERAL REVIEW

2.1. Introduction to Methods of Analysis

The importance of two-phase flows has been mentioned in Chapter 1 and even though two phase flows obey all of the basic laws of fluid mechanics, the equations are always more complicated and more numerous than those for single-phase flows. Several techniques are used for analyzing two-phase flow systems. In ascending order of sophistication they are:

Correlation: This is a technique for obtaining design equations with a minimum of analytical work. Many mathematical correlations performed with modern computers are presented in the literature. The more advanced techniques use dimensional analysis. The major problem with these empirical correlations is that they can be quite misleading if used indiscriminately over a wide range of applications. However, they can be quite satisfactory when applied to conditions similar to those that were used to obtain the data.

Analytical Modelling: Analytical models which do not take account of the details of the flow can be simple and successful in aiding understanding the experimental results as well as predicting the design parameters. For example in the "homogeneous model", the two components of the two-phase flow are treated as a pseudofluid with average properties, without bothering with a detailed description of the flow pattern. In the "separated flow model", the phases are assumed to flow side by side. Separate equations are written for each phase and the interaction between phases is also taken into account, but again, with no detailed description of the flow pattern.

Integral Analysis: The application of this technique starts by assuming the validity of certain functions which may describe various conditions of the flow, e.g. velocity or concentration distributions. These functions are then made to satisfy appropriate boundary conditions as well as the general equations of fluid mechanics stated in an integral form. This is a common method of analyzing problems in boundary layer theories.

Differential Analysis: In this technique the velocity and concentration profiles are deduced from suitable differential equations are are mainly concerned with

local properties of the flow. Some sophisticated versions of this method are able to take into account temporary variations in the system.

To summarize, it can be said that greater accuracy in predicting the results can be achieved by increasing the complexity of the method of analysis. However, this study was concerned with average properties of the flow, and hence the simple analytical model technique was used to analyze the results and make predictions for the behaviour of two phase flow.

2.2. Previous Studies of Two-Phase Flow

Two-phase flow phenomena have been studied for several decades and, although extensive literature is available, it cannot be said that the fluid flow of a mixture of gas and liquid is fully understood.

The earlier investigations were mainly devoted to practical problems of petroleum, chemical and nuclear engineering. The analyses often resulted in empirical correlations which, though sometimes claimed to be general, were often void of physical significance. The following brief review deals only with articles of a general nature and no reference is made to articles which deal only with a specific aspect of a particular liquid gas configuration.

Wallis [1] made an exhaustive review of the work done on two-phase flow. An important contribution was also made by Martinelli, Lockhart and Nelson [2-4] who studied two phase flow pressure drop for the design of boiler tubes, refrigeration systems and condensate-return lines. These studies were devoted especially to the motion of individual phases whereas Zuber and Findlay [5], as well as Smissaert [6] focused their attention on the relative motion of the phases.

Many other studies were done on particular aspects of two-phase flows. Leibson and Coworkers [7] studied the mechanism of formation of bubbles at an orifice. Peebles and Garber [8], and White and Beardmore [9] made extensive studies on the motion of gas bubbles in liquid in order to acquire information for the study of various chemical processes (rectification, absorption, etc.).

All these works have significantly improved the knowledge of multiphase flow, but there still exists numerous gaps in two-phase flow theory. In particular, no study has been made on the effect of reduced pressure on two-phase flow and very little work has been done on non-aqueous systems. Vacuum metallurgy is therefore a new area in the application of two-phase flows.

2.3. Definitions of Terms Used in This Thesis

2.3.1 Flow Patterns

Single-phase fluid flow can be characterized as "laminar" or "turbulent" flow and generally the Reynolds number is sufficient to identify the type of flow. These concepts of laminar and turbulent flow are carried into two-phase flow, however analysis of two-phase flow is more complicated. Based on visual observation, a number of descriptive terms have been established to identify the various types of flow regimes. Figure 2.3.1. illustrates the flow patterns in increasing order of gas flow rate when gas is injected at the bottom of a vertical channel.

The above descriptions are qualitative and somewhat subjective in nature. The same flow pattern is often differently labelled by different observers, and though attempts have been made to avoid this difficulty by specifying ranges of dimensionless groups for each regime, the classification of two-phase flows is still not exact.

2.3.2. Parameters in Two-Phase Flow

The parameters which are used in this study to describe the two-phase flow are:

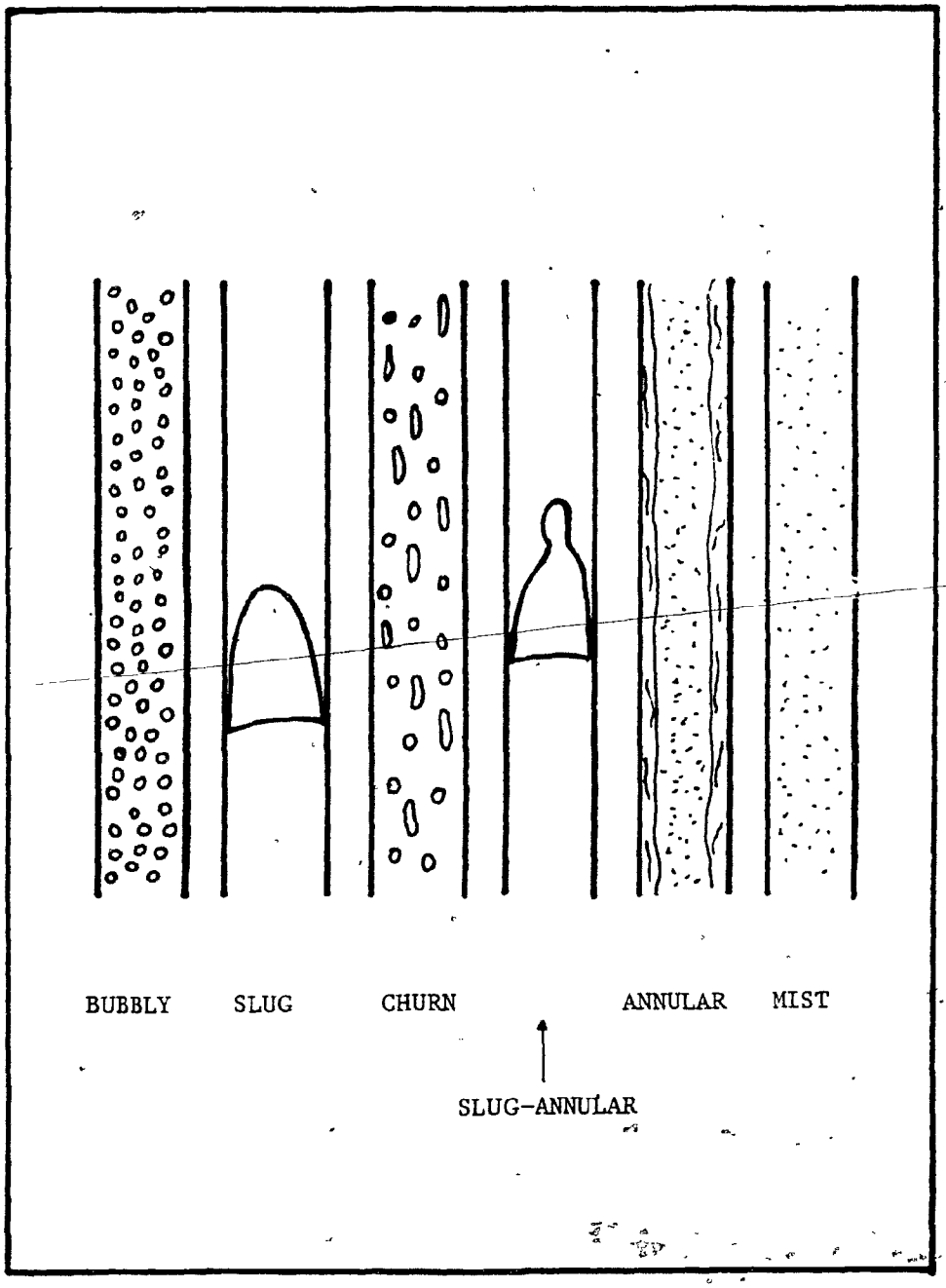

Figure 2.3.1 : Vertical Flow Patterns

a) local velocity

b) relative velocity

c) volume concentration or void fraction

d) volumetric flux density

e) drift velocity

f) volumetric flow rate

In the thesis, the two components of the two-phase flow are distinguished by subscripts 1 and 2. Component 2 was chosen to be the gas phase. In a two-phase flow, every part of the flow field is occupied by one or the other component. Therefore for purposes of analysis, a volume much larger than the bubbles is considered such that this volume contains both phases. The following parameters can then be defined:

a) local velocities $[L.T^{-1}]$

The velocities of the phases with respect to stationary coordinates are represented in any part of the flow by the symbol V. Thus,

V_1 = velocity of the liquid phase

V_2 = velocity of the gas phase

b) relative velocity $[L.T^{-1}]$

The relative velocity between gas and liquid at a particular position in the channel is defined as the difference between the local gas velocity and the local liquid velocity at this position, i.e.:

$$V_r = V_2 - V_1 \qquad (1)$$

c) volume concentration or void fraction

In any particular element of volume larger than the discrete particles (bubbles or drops), the volume concentration or void fraction α, is defined as the fraction of the volume element which is occupied by the gas phase.

d) volumetric flux densities $[L.T^{-1}]$

Volumetric flux densities are represented by the symbol j. They are defined as the surface density over some particular area, A', of the volumetric flux through that area, i.e.

$$j_1 = \frac{V_1 \cdot A'_1}{A'} \qquad \text{volumetric flux density of the liquid} \qquad (2)$$

$$j_2 = \frac{V_2 \cdot A'_2}{A'} \qquad \text{volumetric flux density of the gas} \qquad (3)$$

where A_1' and A_2' represent the areas through which the liquid and the gas are flowing respectively.

$$A_1' + A_2' = A' \tag{4}$$

$$\frac{A_2'}{A'} = \alpha \tag{5}$$

$$j_1 = (1-\alpha)V_1 \tag{6}$$

$$j_2 = \alpha V_2 \tag{7}$$

The volumetric flux density of the mixture is the sum of the individual volumetric flux densities, i.e.,

$$j = j_1 + j_2 \tag{8}$$

e) drift velocities $[L.T^{-1}]$

The drift velocities are defined as the difference between the local velocities and the volumetric flux density of the mixture as follows:

$$V_{1j} = V_1 - j \qquad \text{drift velocity of the liquid} \tag{9}$$

$$V_{2j} = V_2 - j \qquad \text{drift velocity of the gas} \tag{10}$$

f) volumetric flow rates $[L^3.T^{-1}]$

Volumetric flow rates are represented by the symbol Q. The two components are again distinguished by subscripts 1 and 2:

Q_1 = volumetric flow rate of liquid

Q_2 = volumetric flow rate of gas

2.4. The Drift-Flux Model [5]

2.4.1. General Presentation

The drift-flux model is a model in which attention is focused on the relative motion of the gas and liquid phases rather than on the motion of the individual phases. This type of model is often called a "separated flow model". Drift flux theory has widespread application to bubbly, slug and drop regimes of gas-liquid flow. It also has applicability in fluid-particle systems such as fluidized beds. These applications have been reviewed by Wallis.[1]

The theory appearing in this work is based on the work done by Zuber and Findlay [5] who developed a general method which can be used either for predicting the average volumetric concentration (i.e. the average void fraction) or for analyzing and interpreting experimental data. Their analysis takes into account the effect of

non-uniform flow and volume concentration profiles on the local relative velocity between the phases.

2.4.2. Average Velocity and Weighted Mean Velocity of the Gas

For two-phase flow, it is much easier to obtain data on average values than on local ones. Therefore, it is advantageous to consider the average value of any particular quantity, say for example the void fraction α, over the cross-sectional area of the duct, A. This average value $\langle\alpha\rangle$ is defined as:

$$\langle\alpha\rangle = \frac{1}{A} \int_A \alpha \, dA \tag{11}$$

If we consider the local velocity of the gas, V_2, the average velocity of the gas over the total area of the channel is:

$$\langle V_2\rangle = \frac{1}{A} \int_A V_2 \, dA \tag{12}$$

substituting the value of the local velocity V_2 given by Equation (7) in Equation (12), the average velocity of the gas becomes

$$\langle V_2\rangle = \left\langle \frac{j_2}{\alpha} \right\rangle \tag{13}$$

However, it is more convenient to formulate the problem by considering the volumetric flux density of the gas, j_2, instead of the local

velocity of the gas, V_2, the reason for this being that values of Q_2 and A are readily available to a designer or an experimenter.

Hence from Equation (7):

$$\langle j_2 \rangle = \langle \alpha V_2 \rangle = \frac{Q_2}{A} \tag{14}$$

This average value is often referred to as the "superficial" velocity. $\langle j_2 \rangle$ is truly a velocity, but it is in fact the average velocity the gas phase would have if only gas was flowing inside the channel. Since the word "superficial" has no physical meaning, $\langle j_2 \rangle$ will be called the average volumetric flux density.

This and the fact that it can be very difficult to obtain values for $\left\langle \frac{j_2}{\alpha} \right\rangle$, leads us to consider the weighted mean value of the local velocity of the gas. This weighted mean value is:

$$\bar{V}_2 = \frac{\langle j_2 \rangle}{\langle \alpha \rangle} = \frac{\langle \alpha V_2 \rangle}{\langle \alpha \rangle} \tag{15}$$

Substituting V_2 from Equation (10) in Equation (15), we obtain

$$\bar{V}_2 = \frac{\langle \alpha (j + V_{2j}) \rangle}{\langle \alpha \rangle} = \frac{\langle \alpha j \rangle}{\langle \alpha \rangle} + \frac{\langle \alpha V_{2j} \rangle}{\langle \alpha \rangle} \tag{16}$$

Multiplying the numerator and denominator of the first term on the right-hand side of Equation (16) by $\langle j \rangle$, we obtain:

$$\bar{V}_2 = C_o \langle j \rangle + \frac{\langle \alpha V_{2j} \rangle}{\langle \alpha \rangle} \qquad (17)$$

where the distribution parameter, C_o, is defined by:

$$C_o = \frac{\langle \alpha j \rangle}{\langle \alpha \rangle \langle j \rangle} = \frac{\frac{1}{A}\int_A \alpha j \, dA}{\left[\frac{1}{A}\int_A j \, dA\right]\left[\frac{1}{A}\int_A \alpha \, dA\right]} \qquad (18)$$

This expression is applicable to any two-phase flow regime. The analysis takes into account the effects of non-uniform flow and concentration profiles and the effect of the local drift velocity of the gas. Non-uniform flow and concentration profiles are accounted for by the distribution parameter C_o and will be discussed in the next section.

The second term on the right hand side of Equation (17) is the weighted mean drift velocity and will be examined in the following section.

2.4.3. Effects of Non Uniform Flow and Concentration Distribution on the Distribution Parameter, C_o

In a circular channel, the flow and concentration distributions can be expressed as a function of radial position $\frac{r}{R}$ as:

$$\frac{j}{j_c} = 1 - \left(\frac{r}{R}\right)^m \tag{19}$$

and

$$\frac{\alpha - \alpha_w}{\alpha_c - \alpha_w} = 1 - \left(\frac{r}{R}\right)^n \tag{20}$$

The subscripts c and w refer respectively to the values at the center line and the wall of the circular duct of radius R.

Substitution of Equations (19) and (20) in Equation (18) yields:

$$C_o = 1 + \frac{2}{m+n+2}\left[1 - \frac{\alpha_w}{\langle\alpha\rangle}\right] \tag{21}$$

Where C_o is expressed in terms of the volume concentration at the wall, α_w. It can be seen, if the volume concentration is uniform across the duct, i.e., if $\alpha_w = \alpha_c = \langle\alpha\rangle$ that $C_o = 1$. If the volume concentration at the center line is greater than that at the wall, i.e., if $\alpha_c > \alpha_w$, then $C_o > 1$. Finally, if the concentration at the center line is smaller than that at the wall, i.e., if $\alpha_c < \alpha_w$ then, $C_o < 1$.

Figure 2.4.1. shows the values of the distribution parameter C_o as a function of the exponents of the flow and concentration profiles (n, m, in Equations 19, 20) for axisymmetric flow through circular ducts.

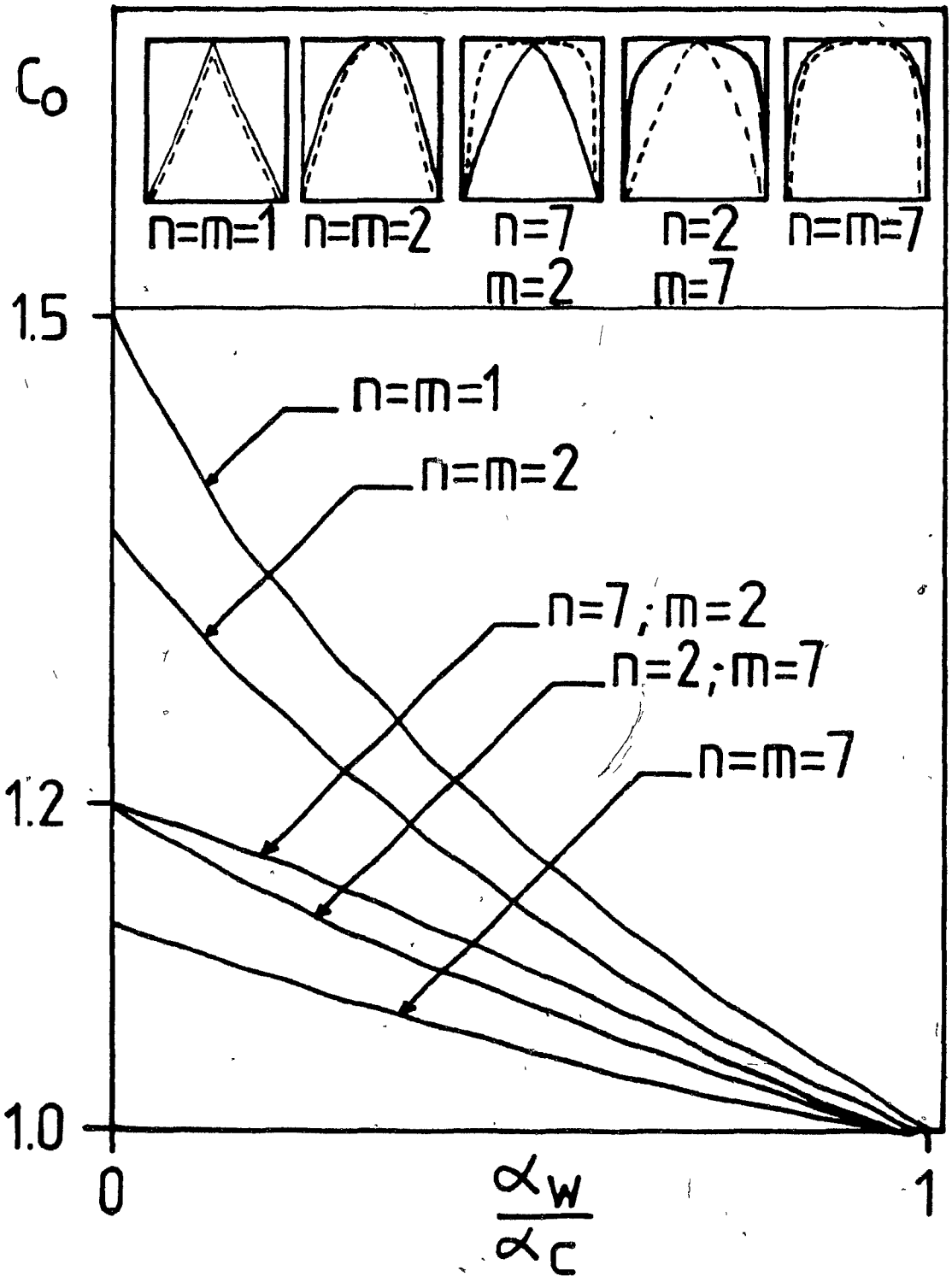

Figure 2.4.1 : Values of the Distribution Parameter, C_o, for Different Concentration Profiles as a Function of $\frac{\alpha_w}{\alpha_c}$. (---- : Concentration Profile, Eq.20)
(—— : Flow Profile, Eq.19)

2.4.4. The Weighted Mean Drift Velocity

The effect of the term $\frac{\langle \alpha V_{2j} \rangle}{\langle \alpha \rangle}$ in Equation (17) is now considered. Recalling that the local drift velocity of the gas given by Equation (10) is the local velocity of a bubble with respect to the local volumetric flux density of the mixture, the simplest analytical expression for this local drift velocity is obtained by assuming that it is unaffected by the presence of other bubbles. This simple expression represents the terminal velocity of a bubble rising in an infinite medium for the slug flow regime and the churn-turbulent bubbly flow, [10-12]. The terminal rising velocity is given by:

$$V_{2j} = 0.35 \left[\frac{g \, \Delta\rho \, D}{\rho_1} \right]^{1/2} \tag{22}$$

for the slug flow regime ($\Delta\rho = \rho_1 - \rho_2$, D = diameter of duct)

and

$$V_{2j} = 1.53 \left[\frac{\sigma g \, \Delta\rho}{\rho_1^2} \right]^{1/4} \tag{23}$$

for the churn-turbulent bubbly flow ($\Delta\rho = \rho_1 - \rho_2$, σ = surface tension).

The validity of Equation (22) has been discussed by White and Beardmore [9]. They also present expressions for the terminal velocity of a slug when viscous effects become important. The value of the constant in Equation (23), 1.53, is that proposed by Harmathy [13] whereas Peebles and Garber recommend a value of 1.18 [8]. Both values are approximations and Equation (23) is useful since it shows

that, in this type of flow, the rise velocity is independant of the bubble diameter.

When the presence of other bubbles affects the motion of a given bubble, the local drift velocity will depend on the concentration. In general, the local drift velocity can be expressed in the form of

$$V_{2j} = v_\infty (1 - \alpha)^k \qquad (24)$$

Using the volume concentration as given by Equation (20), the weighted mean drift velocity can be calculated by integrating $\int_A \alpha(1-\alpha)^k \, dA$. This general expression was not used in this work.

2.4.5. Summary of the Drift-Flux Model

1. The weighted mean velocity of the gas phase is given by

$$\bar{V}_2 = C_o \langle j \rangle + \frac{\langle \alpha \, V_{2j} \rangle}{\langle \alpha \rangle} \qquad (17)$$

2. The value of C_o depends on flow and concentration profiles:

   - In axisymmetric two-phase flow, it may range from about 1.5 to 1.0 when $\alpha_w < \alpha_c$

- it is smaller than unity, i.e., $C_o < 1$ when $\alpha_w > \alpha_c$

3. For slug-flow regime

$$\bar{V}_2 = C_o \langle j \rangle + 0.35 \left[\frac{g.\Delta\rho.D}{\rho_1} \right]^{1/2}$$

4. For churn-turbulent bubbly flow

$$\bar{V}_2 = C_o \langle j \rangle + 1.53 \left[\frac{\sigma.g.\Delta\rho}{\rho_1^2} \right]^{1/4}$$

2.5. Metallurgical Applications of Gas Injection

Gas bubble-liquid metal interactions are important in numerous refining processes such as the deoxidation of copper, degassing of aluminium, and decarburization of high alloy and stainless steels. Many investigations have been carried out on various aspects of gas injection into liquid metals and many of these works are summarized by Szekely and Themelis [14].

Among the numerous studies of gas injection, the Gas-Lift Mixing Reactor (GMR) process for the desulphurization of Molten Pig iron was investigated at Kobe Steel by Narita and co-workers [15]. Their process is based on the injection of gas into pig iron at the

bottom of a cylindrical vertical lifting tube immersed in the liquid pig iron. The buoyancy of the rising bubbles is the driving force for lifting the molten pig iron through the tube. The lifted hot metal overflows the top of the tube and falls back onto a desulphurizing agent layer which had been added to the surface of the liquid metal. By this means Kobe Steel improved the desulphurization of the pig iron.

A similar process based on the principle of gas-lift pump was developed by Harris [16] with the purpose of enhancing the vacuum refining kinetics of molten metals. The outline of the process is shown in Figure 2.5.1. Here again, in this process known as "Lift-Spray Vacuum Refining," the injection of gas at the bottom of the lifter tube lifts the liquid from beneath the bath surface to a point above the bath surface. At the lifter "overflow", that is the top of the channel, the liquid is dispersed in the vacuum by the action of the gas bubbles exploding into the vacuum, and thus creating very large surface areas for evaporation. It is also clear that a great amount of melt turbulence is created. Consequently, melt phase resistance is expected to be quite low and the injection of gas is also hoped to lower the gas phase mass transport since the injected gas will convect evaporated vapour away from the liquid metal. A Lift-Spray system also creates fresh metallic surface exposed to vacuum.

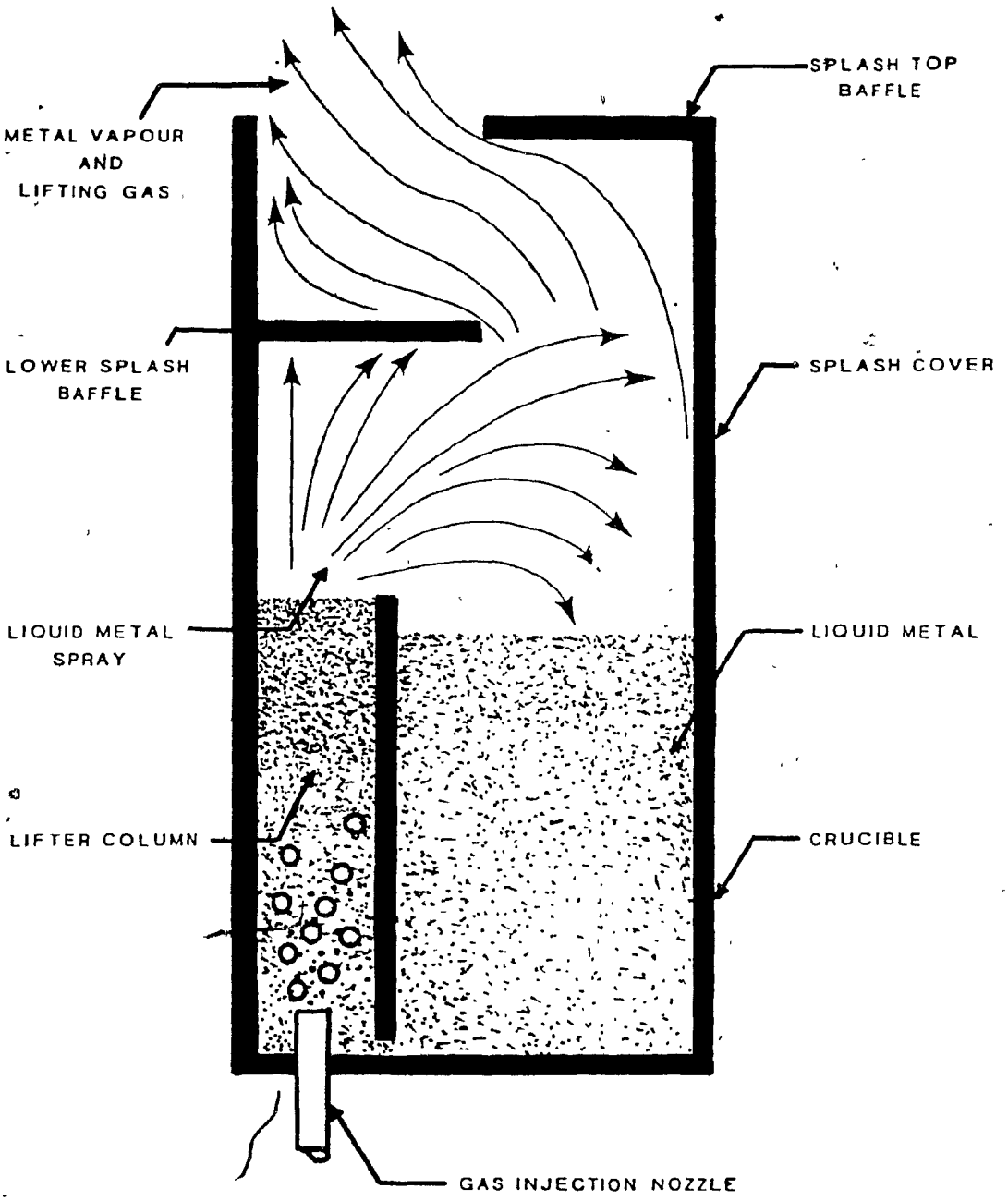

Figure 2.5.1 : Schematic Representation of a Lift-Spray System, after Harris [16] .

It is the purpose of the present study to quantify the effect of vacuum on two-phase flows as well as on lift and overflow rates as a function of the various design and operation parameters. A cold model using water was assembled for this purpose and is shown in Figure 2.5.2.

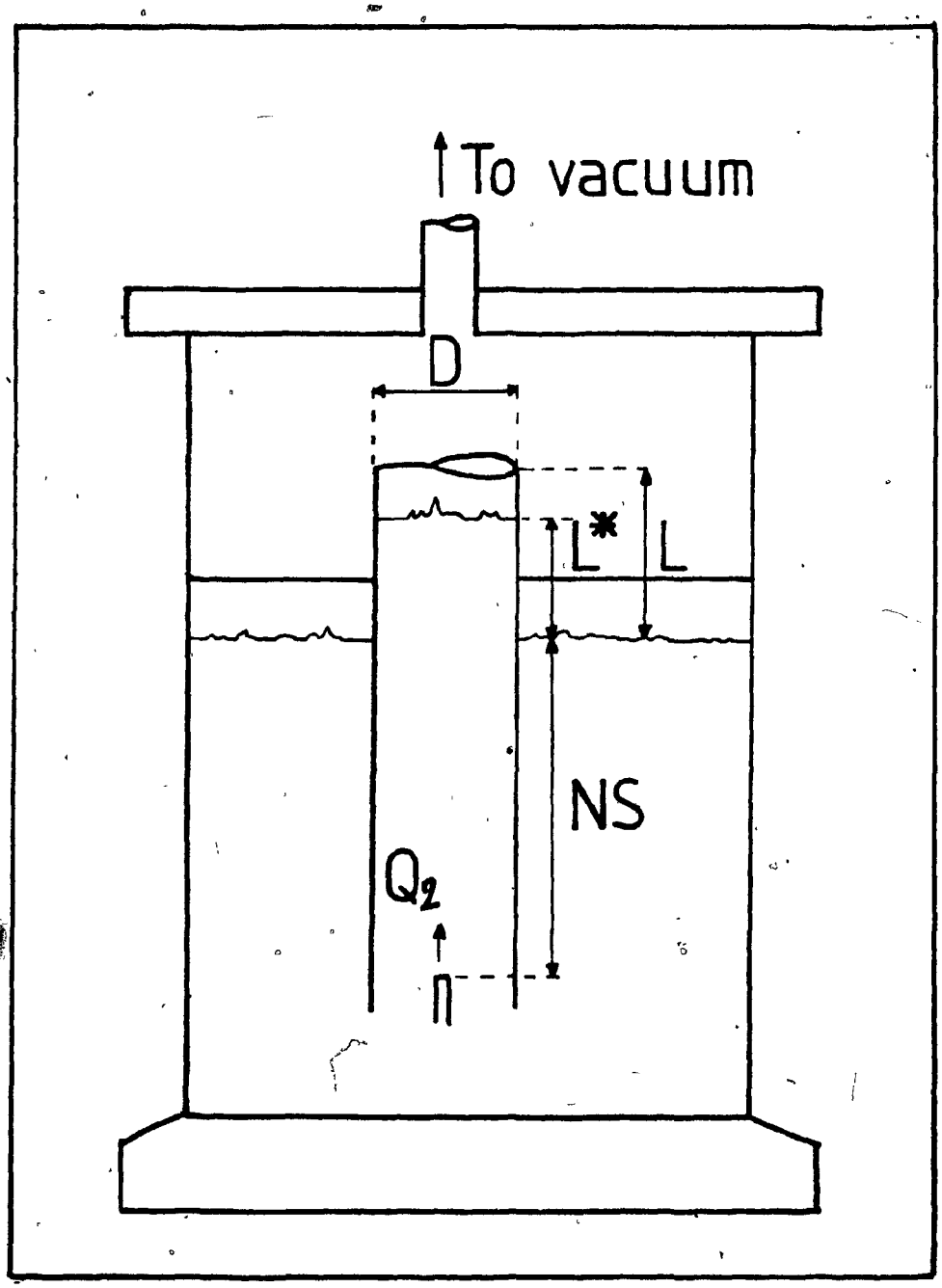

Figure 2.5.2 : Schematic representation of Experimental Apparatus with Relevant Dimensions Labelled.

CHAPTER THREE

EXPERIMENTAL

3.1. Introduction

The aims of the experimental program were:

(i) to visualize two phase flow through a lifter under vacuum and,

(ii) to correlate the liquid flow rate to various experimental parameters.

The experimental program was broken into two parts. In the first, the interaction of the gas and liquid phases was observed and studied qualitatively by means of examining slow motion films of the turbulent flow. The films aided in understanding the various regions of flow phenomena by showing that a churn-turbulent flow pattern was established for any constant gas flow rate greater than about 20 cm^3/S. In the second part, experiments were conducted in order to establish the experimental parameters of the drift flux model (C_o and v_∞) and then verify the validity of the energy balance applied to the lift-spray system (see Chapter 6).

The first set of quantitative experiments was carried out with no net flow of the liquid phase. The distribution parameter and

terminal velocity were then derived from measurements of the maximum lift. The second set of quantitative experiments was carried out with liquid overflow and liquid overflow rate was correlated against the various experimental parameters.

3.2. Experimental Variables

Previous studies have suggested that a number of experimental variables influence the two-pnase flow. In the case of a Lift-Spray system or in any similar apparatus the following variables can have an influence:

(a) Properties of the liquid phase:

(a-1) Density ρ_1

(a-2) Temperature T_1

(a-3) Viscosity σ_1

(b) Properties of the gas phase:

(b-1) Density ρ_2

(b-2) Temperature T_2

(b-3) Viscosity σ_2

(c) Surface tensions (between liquid and gas, liquid and container and gas and container).

(d) Cross-sectional area of lifter

(e) Length of lifter (above and under liquid)

(f) Location of nozzle or nozzles (e.g. centered/offset etc.)

(g) Other geometry of system:

(g-1) Inclined lifter

(g-2) Non-cylindrical lifter

(g-3) Lifter overflow design, etc.

(h) Gas flow rate

(i) Top pressure

(j) Pulsed gas flow

The importance of the first three parameters, the physical properties of the components, has been shown in the previous chapter. The effects of these parameters are well known and taken into account in the determination of C_0 and v_∞. No attempt was made in this study to vary the properties of the liquid and the gas phases (only water and nitrogen were used).

Of the remaining parameters, d, e, h, and i were investigated extensively. The system geometry, f and g, which was employed, was chosen in order to simplify the problem. Pulsed flow, j, was examined briefly in the photographic studies.

3.3. Experimental Apparatus

A glass cylinder 120 cm high and 45 cm I.D., mounted on and sealed to a steel plate was used to contain the water. The container was divided into two sections having different volumes by a horizontal plexiglass divider plate 1/2" thick. This plate could be moved up and down and was sealed to the glass with a rubber ring.

This plate was used to hold and position the lifter and to collect the overflowing water in the top section (see Figure 3.3.1.).

A plexiglass plate 1" thick was sealed tightly on top of the glass cylinder in order to be able to apply vacuum to the system. The top plate was designed with lifting gas inlet, vacuum outlet, and water recirculation ports.

The circulation of the water from the top container to the bottom was made possible by a submersible pump with a maximum capacity of approximately 2000 cm^3/S. The water flow rate as well as the gas flow rate were measured with rotameters. The corresponding calibration curves are shown in Figures 3.3.2. and 3.3.3. The pressure inside the system and the pressure on the gas line at the rotameter were both measured with a mercury column-type manometer. The gas flow rate, the recirculated water flow rate and the top pressure were controlled by separate valves.

3.4. Experimental Parameters

The parameters which were controlled during the experimental investigation were:

- Cross-sectional area of lifter
- Length of lifter above free surface of liquid
- Nozzle submergence

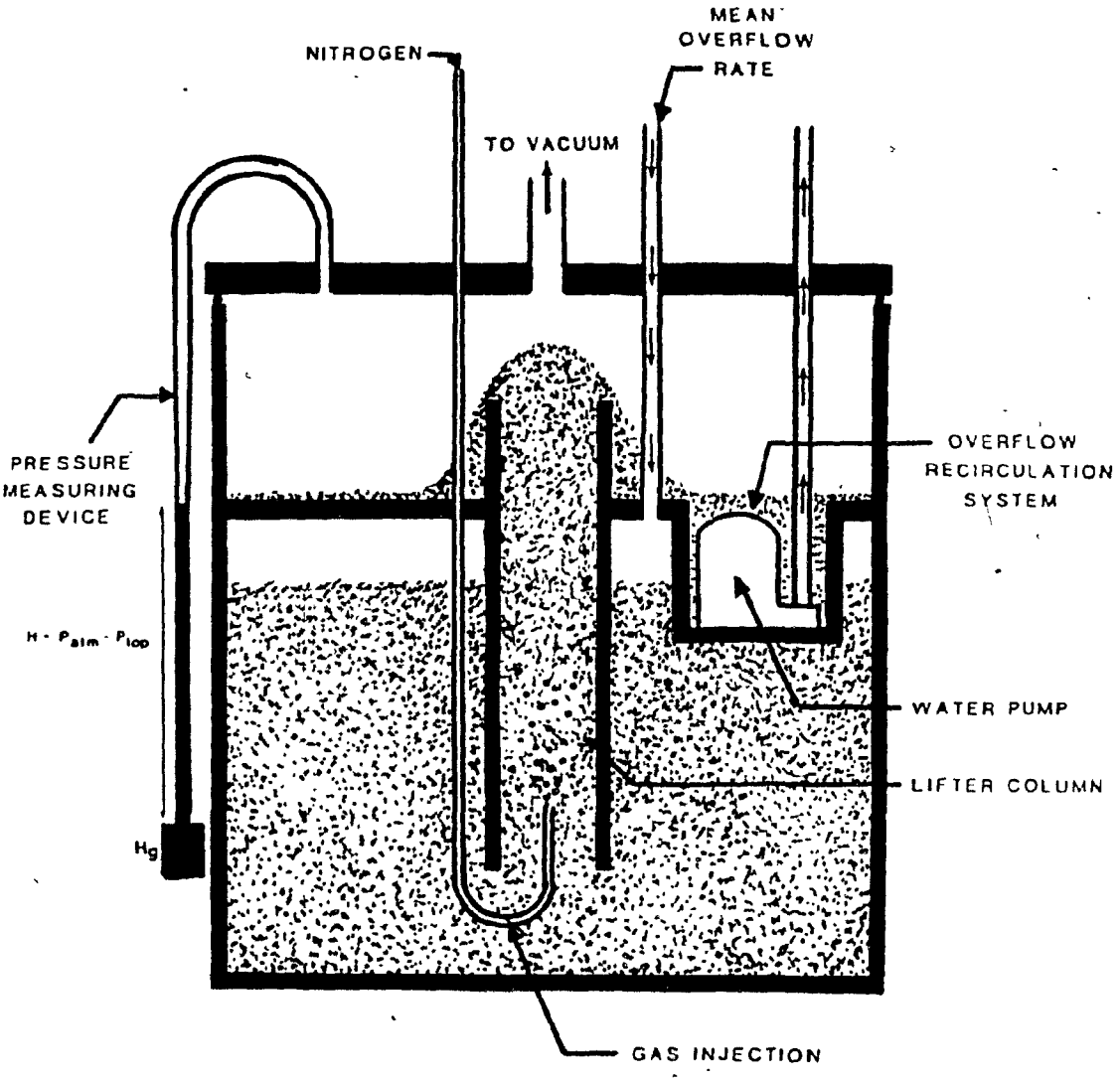

Figure 3.3.1 : Schematic Representation of Experimental Apparatus.

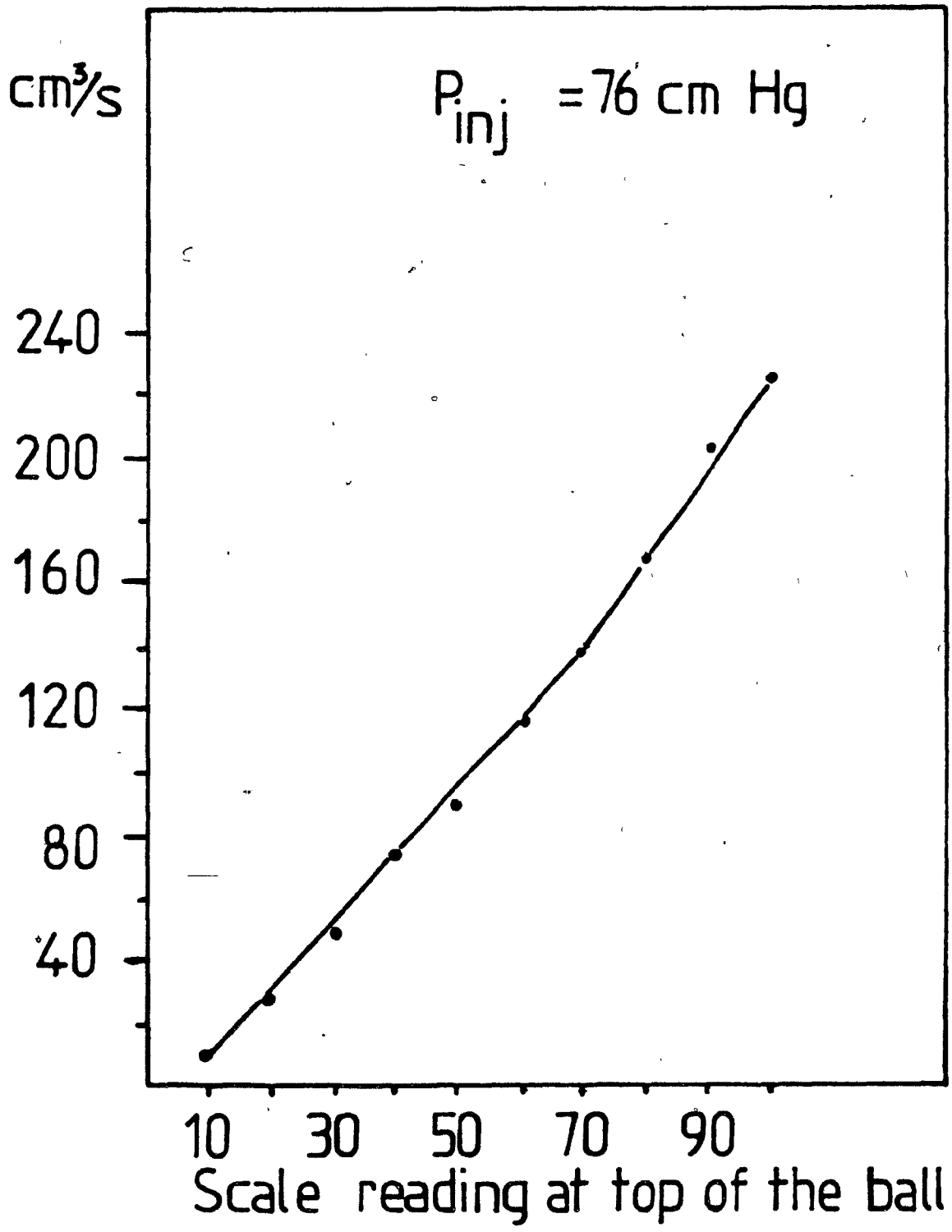

Figure 3.3.2 : Calibration Curve for the Rotameter Measuring the Injected Gas Flow Rate.

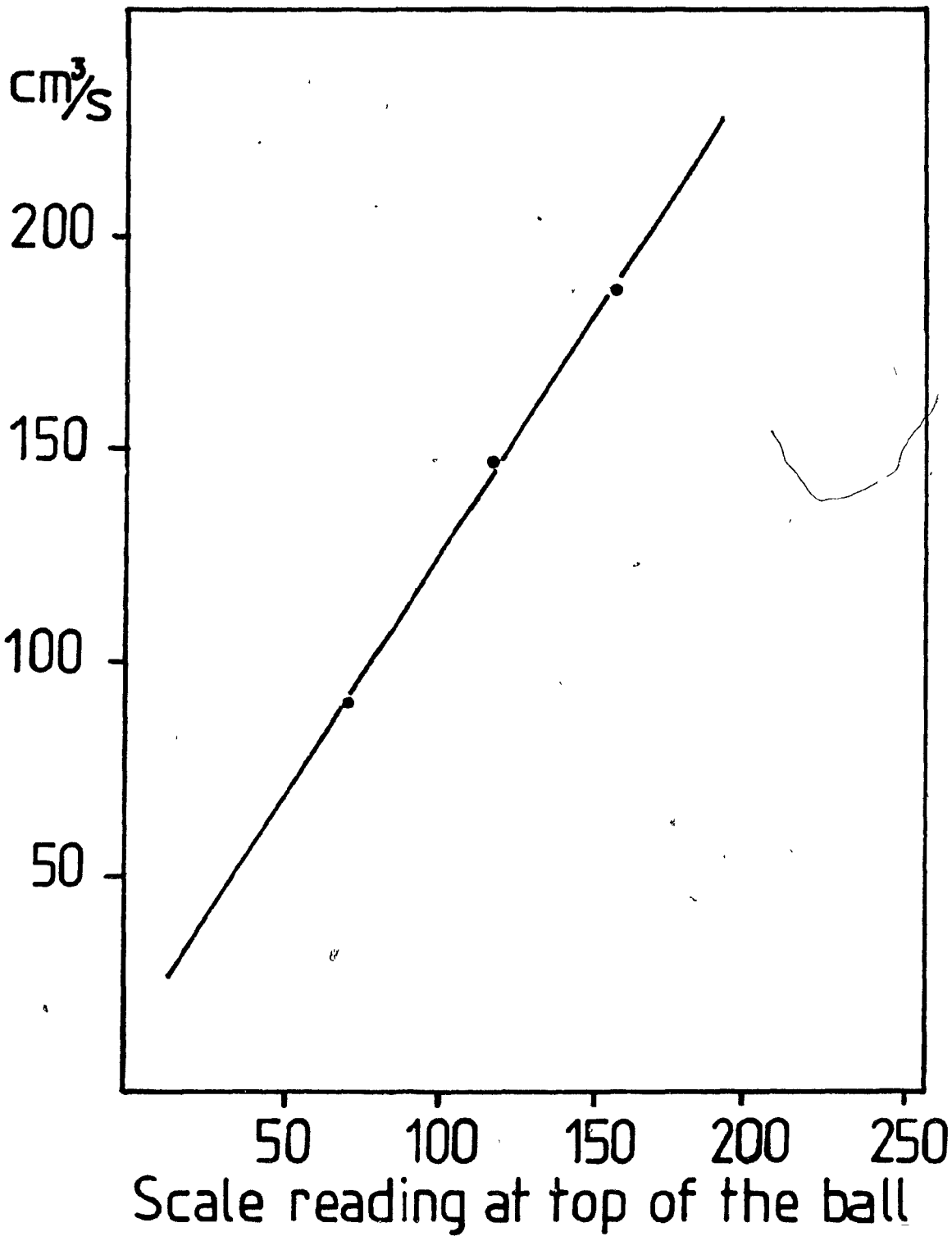

Figure 3.3.3 : Calibration Curve for the Rotameter Measuring the Water Flow Rate.

- Gas flow rate
- Top pressure

The ranges of these parameters were:

CROSS-SECTIONAL AREA OF LIFTER:

This was a discreet variable with values of 36.3 cm^2, 55.4 cm^2, 113.1 cm^2. These values correspond to the three different tubes used in the experiments, i.e. 3" O.D., 4" O.D. and 5" O.D. tubes.

LENGTH OF LIFTER ABOVE FREE SURFACE OF LIQUID:

15cm to 30 cm. This length remained at its maximum value during the lift experiments in order to avoid the liquid overflow. This maximum limit was set by the experimental apparatus.

NOZZLE SUBMERGENCE:

45 cm to 75 cm. Again, the maximum value was set by the dimension of the experimental apparatus.

GAS FLOW RATE (stp):

The lower limit was the minimum gas flow rate which could establish a churn-turbulent type of two-phase flow, about 20 cm^3/s.

The upper limit was determined by the maximum capacity of the rotameter used to measure the flow rate, about 225 cm^3/s.

TOP PRESSURE:

The lower limit was the minimum pressure attainable without boiling the water. Vapor pressure of water at 25°C being almost 24 mm of Hg, the minimum value used in the experiments was roughly 3 x 10 mm of Hg. The maximum value was 760 mm Hg (atmospheric pressure).

3.5. Experimental Procedure

3.5.1. Slow Motion Movies

The movies were made using a Locam 16 mm variable frame speed camera fitted with a Cosmicar 22.5-95 mm F 1.5 television zoom lens. The film speed used was 30 frames per second. Movies of continuous and pulsed flows were made.

3.5.2. Lift Experiments

The glass container was filled with tap water. This water was renewed for each set of experiments to minimize the contamination of the water with rust forming on the steel plate.

The divider plate was placed inside the container after the lifter and the gas injector has been connected to it. The gas line was connected from the injector to gas inlet. The top was sealed and vacuum applied.

Gas flow rate was set to a predetermined value and the top pressure was controlled by a manual valve. Great care was taken in all experiments to ensure that:

(i) no water overflowed the lifter and,

(ii) both top pressure and gas flow rate remained constant.

The height reached by the two-phase mixture in the tube was measured against graduations on the side of the lifter. The main advantage of the procedure described is that it was possible to gather a large number of data for a given system, that is, fixed nozzle submergence and area of lifter, by varying the top pressure and gas flow rate.

3.5.3. Overflow Experiments

The set up of overflow experiments was the same as in the lift experiments. The only difference was that the recirculation lines for water were also connected.

After the system was sealed and the vacuum created, the gas flow rate was set and the top pressure was controlled. Again, a great care was taken to ensure that:

(i) overflow occurred and,

(ii) both top pressure and gas flow rate remained constant

The water recirculation rate was controlled by controlling the pumping rate of the pump to keep the same level of water on both sides of the plexiglass plate and at the steady state the overflow rate was given by the water rotameter Unfortunately, overflow rates much higher than the pump capacity (see Figure 3.3.3.) were reached. In these cases the overflow was determined by measuring the time required for the lifter to carry 1500 cm^3 of water from below the divider plate to the section above the divider plate (i.e. a decrease of 1 cm of water in the lower section). This was not believed to disturb the experimental conditions.

3.6. Precision of Measured Data

The major difficulty of this experimental work was simultaneous regulation of the flow rates of gas and liquid when using the submersible pump while at the same time maintaining steady state. Once steady state was achieved measurements were easily taken. This was not the problem with the fixed overflow volume technique, but here the measurements had to be taken very rapidly.

An approximate value of the absolute error for each parameter is given in Table 3.6.1.

Another source of error was the variation in local properties in a two-phase flow system. In other words, the level of lift in the non-overflow experiments was constantly oscillating up and down, and the overflow rate in the overflow experiments was also varying periodically. Therefore, the recorded values for lift and overflow were averaged over a definite period of time. No further consideration of these instabilities was taken.

3.7. Summary

In summary, the experiments were aimed at measuring lifts and overflow rates in a Lift-Spray system under vacuum. Photographic observations led to a better understanding of the two phase flow under vacuum and helped in understanding the influence of the various experimental parameters. Variation in flow rate of gas, area of duct, top pressure and nozzle submergence were taken into account for the interpretation of the results whereas oscillation of the system was a source of experimental uncertainty.

VARIABLE	VARIABLE SYMBOL	RANGE	ERROR (+/-)
Top Pressure	P_{TOP}	3-76 cm Hg	0.5 cm Hg.
Gas Flow Rate	Q'_2	26-225 cm^3/s STP	2 cm^3/s
Gas Injection Pressure	P_{INJ}	66-86 cm Hg	0.2 cm Hg
Nozzle Submergence	NS	45-75 cm	0.5 cm
Lifter Length	L	15-30 cm	0.5 cm
Lift Height	L*	0-30 cm	0.5 cm
Water Overflow Rate	OVFL OR Q_1	52-3000 cm^3/s	leaks

Table 3.6.1. Approximate value of the absolute error for each parameter.

CHAPTER FOUR

PHOTOGRAPHIC STUDIES

4.1. Introduction

This chapter presents photographs of the gas-liquid mixture in the lifter and the flow of liquid at the top of the lifting tube. The photographs are selected frames from 16mm cine films.

4.2. Flow Patterns Under Vacuum

At low gas flow rate, the flow pattern was typical of a laminar bubbly flow as shown in Figure 4.2.1. When the gas flow rate was increased, the frequency of the bubble formation first increased, and then the volume of the bubbles increased to form spherical caped bubbles. Figure 4.2.2. shows such a bubble. This type of behavior has been reported in many investigations and no attention was paid in this study to determine the ranges of gas flow rate for such flow patterns.

When the gas flow rate was higher than about $20cm^3/s$ the flow pattern was typical of a churn-turbulent bubbly flow so long as the gas injection was continuous. See Figures 4.2.3. to 4.2.5.

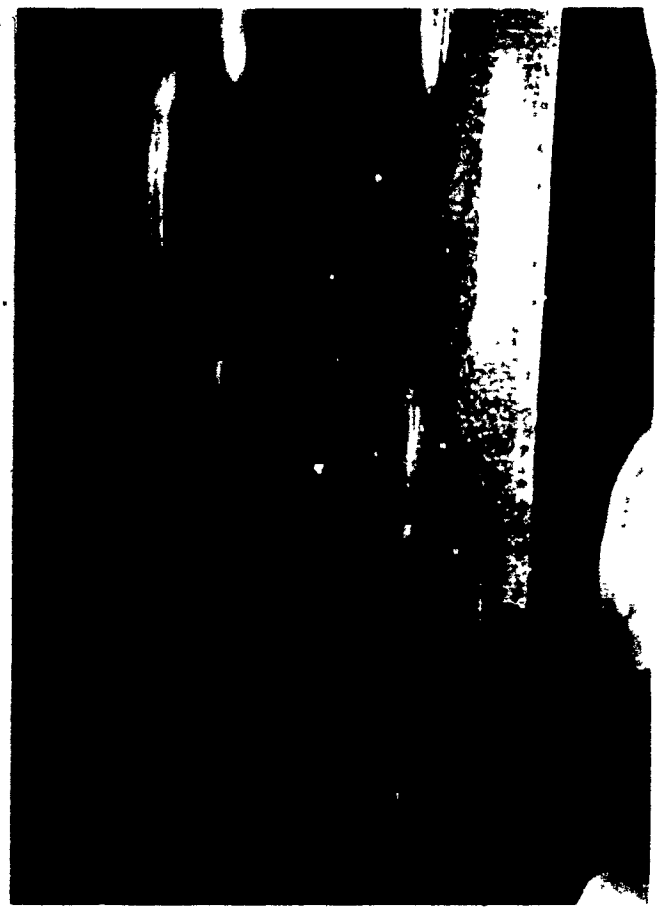

4.2.1. Laminar Bubbly flow

(O.D = 4", NS = 40 cm, L = 50 cm, Q_2 = 20 cm^3/s, P_{TOP} = 76 cm Hg)

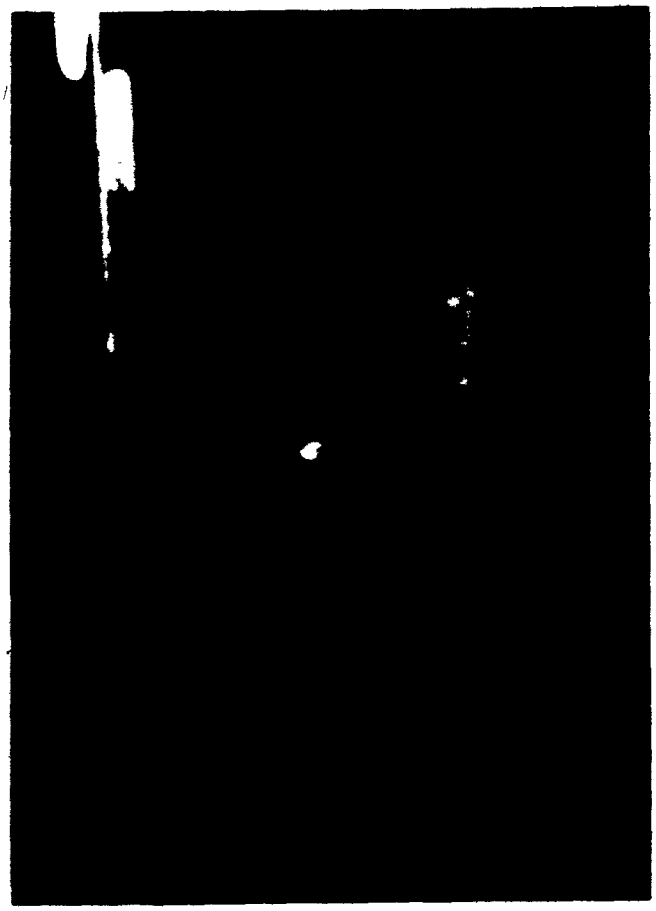

4.2.2. Spherical cap bubble

4.2.3. Churn-Turbulent bubbly flow

(O.D = 4", NS = 40 cm, L = 50 cm, Q_2 = 200 cm^3/s, P_{TOP} = 76 cm Hg)

4.2.4. Churn-Turbulent bubbly flow

(O.D = 4", NS = 40 cm, L = 50 cm, Q_2 = 500 cm^3/s, P_{TOP} = 76 cm Hg)

4.2.5. Churn-Turbulent bubbly flow

(O.D = 4", NS = 40 cm, L = 50 cm, Q_2 = 1500 cm^3/s, P_{TOP} = 76 cm Hg)

Slug flows were observed only when the gas injection was periodic, i.e. when the gas line was alternatively opened and closed. This way, the formation of very large slugs was made possible as shown in Figure 4.2.6. This type of pulsating injection flow rate was not studied further but it could be an interesting alternative for recirculating a liquid in this type of gas-liquid pump.

4.3. The Liquid Overflow

For continuous gas injection at flow rate of gas higher than about 20 cm^3/s, the flow regime was characteristic of a churn-turbulent bubbly flow. Pictures were taken at the lifter overflow and compared with photographs of a similar design used in liquid aluminium [16] as shown in Figures 4.3.1. and 4.3.2. The visual observation shows a very similar behavior of the overflow in the Nitrogen-Water System when compared to the Nitrogen-Aluminium one. In both systems a frequent inward collapse of the Liquid film into the lifter was also notice. From a visual point of view, the gas-lifter system seemed to be a reasonable model of the gas-liquid metal system.

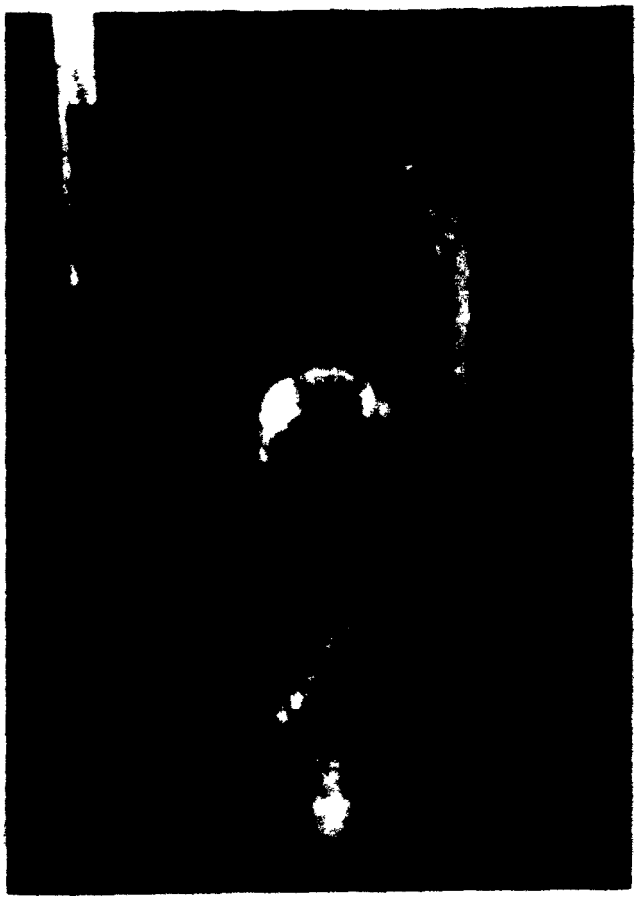

4.2.6. Slug flow

(No experimental data; the size of such bubbles could reach 1500 cm^3)

4.3.1. Aluminum Overflow

4.3.2. Water Overflow

(O.D = 4", NS = 40 cm, L = 50 cm, Q_2 = 2500 cm^3/s, P_{TOP} = 10 cm Hg)

CHAPTER FIVE

RESULTS

5.1. Measurements in Lift Experiments

The parameters which were measured in the lift experiments were:

(a) Pressure on the gas line, P_{INJ}

(b) Nozzle Submergence, NS

(c) Top Pressure, P_{TOP}

(d) Gas flow rate, Q_2, as read from the rotameter

(e) Lift, L*, as measured from the free surface of the liquid to the top of the two-phase mixture in the column.

These measurements are tabulated for the experiments on 3, 4, and 5" outside diameter (i.e. 6.8, 9.3, 12.0 cm I.D.) tubes in Tables 5.1.1. to 5.1.3.

5.2. Measurements in Lift-Overflow Experiments

The parameters which were measured in the Lift-Overflow experiments were the same as those measured in the Lift experiments with the exception of L*. Here, the length of the tube above the liquid surface is taken as the lift height. In addition, the rate at which water flowed through the lifter was also determined as described in Chapter 4. Thus, the parameters measured were:

Exp. Number	P_{INJ} (cm Hg.)	NS (cm)	P_{Top} (cm Hg)	Q'_2 (cm^3/s)	L* (cm)
1-A	87.0	54.0	10	29.0	11
2-A	83.5	54.0	19	109.5	18
3-A	86.0	54.0	20	26.5	6
4-A	84.8	54.0	20	62.0	11
5-A	83.5	54.0	19	172.5	28
6-A	85.8	54.0	30	66.5	8
7-A	87.5	54.0	30	22.0	3
8-A	83.0	54.0	30	134.5	15
9-A	82.5	54.0	30	200.5	21
10-A	87.0	54.0	40	26.0	3
11-A	85.3	54.0	40	68.5	6
12-A	84.0	54.0	40	128.0	12
13-A	82.5	54.0	40	200.5	18
14-A	86.5	54.0	50	27.5	2
15-A	84.0	54.0	50	73.0	6
16-A	83.5	54.0	50	116.0	9
17-A	82.5	54.0	50	189.0	13
18-A	87.0	54.0	76	29.0	1
19-A	85.3	54.0	76	71.0	4
20-A	82.7	54.0	76	122.0	6
21-A	87.0	54.0	76	170.0	8
22-A	86.2	54.0	76	198.0	10

Table 5.1.1. Measured Values of Experimental Parameters and Lift in a 3" (6.8 cm I.D.)

Exp. Number	P_{INJ} (cm Hg)	NS (cm)	P_{TOP} (cm Hg)	Q'_2 (cm^3/s)	L* (cm)
1-B	76.0	48.0	5	123.0	30
2-B	83.0	48.0	10	22.0	5
3-B	77.5	48.0	10	73.0	10
4-B	75.5	48.0	10	142.0	17
5-B	74.5	48.0	10	214.0	26
6-B	81.5	48.0	20	26.0	2
7-B	77.5	48.0	20	76.0	6
8-B	75.5	48.0	20	153.0	10
9-B	74.0	48.0	20	214.0	14
10-B	80.5	48.0	30	40.0	3
11-B	77.8	48.0	30	78.5	4
12-B	81.0	48.0	30	200.0	1
13-B	86.5	48.0	40	38.0	2
14-B	84.0	48.0	40	81.0	4
15-B	81.0	48.0	40	142.0	6
16-B	79.5	48.0	40	208.0	9
17-B	85.0	48.0	50	48.0	2
18-B	82.5	48.0	50	96.0	4
19-B	81.0	48.0	50	158.0	5
20-B	79.8	48.0	50	212.0	7
21-B	85.5	48.0	76	40.0	1
22-B	82.3	48.0	76	86.0	2
23-B	82.5	48.0	76	132.0	3
24-B	86.5	48.0	76	214.0	5

Table 5.1.2. Measured Values of Experimental Parameters and Lift in a 4" Tube (9.3 cm I.D.)

Exp. Number	P_{INJ} (cm Hg)	NS (cm)	P_{TOP} (cm Hg)	Q_2' (cm^3/s)	L* (cm)
1-C	87.0	48.0	5	22.0	6
2-C	83.5	48.0	4	76.0	18
3-C	83.5	48.0	4	128.0	24
4-C	80.5	48.0	5	204.0	29
5-C	87.2	48.0	10	28.0	4
6-C	83.5	48.0	10	78.5	7
7-C	83.3	48.0	10	114.0	11
8-C	80.5	48.0	10	204.0	13
9-C	86.5	48.0	20	24.5	2
10-C	83.8	48.0	20	73.0	4
11-C	82.5	48.0	19	145.0	8
12-C	81.0	48.0	20	218.0	12
13-C	87.0	48.0	30	31.0	1
14-C	84.5	48.0	30	80.0	3
15-C	82.0	48.0	30	148.0	5
16-C	81.0	48.0	30	212.0	7
17-C	83.0	48.0	40	136.0	4
18-C	80.3	48.0	40	220.0	6
19-C	85.0	48.0	76	123.0	2
20-C	87.0	48.0	76	220.0	3

Table 5.1.3. Measured Values of Experimental Parameters and Lift in a 5" Tube (12.0 cm I.D.)

(a) Pressure on the gas line, P_{INJ}

(b) Nozzle Submergence, NS

(c) Top pressure, P_{TOP}

(d) Length of lifter above liquid surface, L

(e) Gas flow rate, Q_2', as read from the rotameter

(f) Overflow rate, OVFL

These measurements are tabulated in Table 5.2.1 for overflow experiments for at 3" Tube (6.8 cm I.D.). Most of the measurements were done without the use of the submersible pump (see Chapter Three). An asterisk indicates the values measured with the use of the pump. No measurements of the overflow rate were made in larger diameter tubes because overflow situations were difficult to reach due to the limitations of the apparatus.

Exp. Number	P_{INJ} (cm Hg)	NS (cm)	P_{TOP} (cm Hg)	L (cm)	Q'_2 (cm^3/s)	OVFL (cm^3/s)
1-D	91.0	68.0	3.5	20.8	16	72
2-D	85.0	66.0	4.0	22.8	116	1570
3-D	80.5	67.5	9.0	21.3	148	1064
4-D	83.0	67.0	11.5	21.8	116	174
5-D	81.0	69.5	13.5	19.3	146	560
6-D	77.2	69.5	18.0	19.3	181	424
7-D	73.0	65.5	18.0	23.3	212	455
8-D	94.0	69.0	20.0	19.8	170	314
9-D	88.0	68.2	29.0	20.6	222	62
10-D	76.5	68.5	15.0	20.3	159	490
11-D	73.0	67.5	15.0	21.3	192	424
12-D	83.0	68.0	12.0	20.8	118	200*
13-D	74.0	70.8	30.0	18.0	222	138*
14-D	86.0	69.2	10.0	19.6	98	176*
15-D	89.5	66.5	4.0	22.3	33	143*
16-D	86.0	68.5	9.0	20.3	76	103*
17-D	81.7	68.8	15.0	20.0	136	179*
18-D	76.0	69.5	21.5	19.3	184	147*
19-D	85.3	73.5	3.0	15.3	162	2690
20-D	87.5	70.5	4.0	18.3	138	1962
21-D	86.5	73.5	4.0	15.3	138	3139
22-D	87.5	65.8	3.0	23.0	114	1189
23-D	86.5	68.3	5.0	20.5	132	1054
24-D	82.0	68.5	6.5	20.3	180	1347
25-D	82.5	71.3	7.0	17.3	184	2092
26-D	81.0	70.5	10.0	18.3	203	1327
27-D	84.0	68.0	7.0	20.8	162	975
28-D	78.5	69.5	9.0	19.3	208	1171
29-D	84.0	71.5	8.0	17.3	167	1635
30-D	86.5	71.5	11.0	17.3	138	1046
31-D	84.5	72.5	14.0	16.3	167	923
32-D	85.0	71.5	12.0	17.3	158	1021

Table 5.2.1. Measured Values of Experimental Parameters and Overflow Rates in a 3" Tube.

CHAPTER SIX

METHODS OF ANALYSIS OF LIFT/LIFT-OVERFLOW DATA: A NEW MODEL FOR OVERFLOW PREDICTION

6.1. The Drift-Flux Model as Applied to Lift Experiments

The distribution parameter C_o and the weighted mean drift velocity, $\frac{\langle a V_{2j} \rangle}{\langle a \rangle}$, can be easily calculated from the height of the water-gas column in experiments where there was no overflow. The reasoning and method were as follows:

The average volumetric flux density of the mixture, $\langle j \rangle$ was that of the gas alone because there was no net flow of water.

Thus, $Q_1 = OVFL = 0$

therefore from equations (8) and (14):

$$\langle j \rangle = \frac{Q_1 - Q_2}{A} = \frac{Q_2}{A} \qquad (25)$$

The weighted mean velocity is then given from Equation (15) by:

$$\bar{V}_2 = \frac{\langle j_2 \rangle}{\langle a \rangle} = \frac{Q_{2/A}}{\langle a \rangle} \qquad (26)$$

where the average void fraction, $\langle\alpha\rangle$, when there is no overflow, is given by:

$$\langle\alpha\rangle = \frac{L^*}{L^* + NS} \tag{27}$$

L* is the level reached by the gas-liquid mixture inside the lifter as measured from the still bath surface (see Figures 2.5.2. and 5.2.1.).

$\langle\alpha\rangle$ in this work is an average value across the cross sectional area of the tube as well as long the length of the column. Q_2 is also an average along the length of the channel. This will be discussed later.

Substituting Equation (27) in Equation (26) yields an expression for the weighted mean velocity of the gas $\bar{V}_2$:

$$\bar{V}_2 = \frac{Q_2}{A} \times \frac{L^* + NS}{L^*} \tag{28}$$

$\bar{V}_2$ can then be plotted as a function of $\langle j\rangle$ and from Equation (17), C_o and $\frac{\langle\alpha V_{2j}\rangle}{\langle\alpha\rangle}$ can be determined from the slope and intercept, respectively, i.e.:

$$\bar{V}_2 = C_o \langle j\rangle + \frac{\langle\alpha V_{2j}\rangle}{\langle\alpha\rangle} \tag{17}$$

this can be stated using Equations (25) and (28) as:

$$\frac{Q_2}{A} \times \frac{L^* + NS}{L^*} = C_o \times \frac{Q_2}{A} + \frac{\langle \alpha V_{2j} \rangle}{\langle \alpha \rangle} \qquad (29)$$

where $\frac{\langle \alpha V_{2j} \rangle}{\langle \alpha \rangle}$ is the terminal velocity of the gas, V_∞, in the case of a churn-turbulent bubbly flow or in a slug flow regime.

6.2. The Drift-Flux Model as Applied to Lift-Overflow Experiments

For Lift-Overflow experiments, Equation (17) can be written as:

$$\bar{V}_2 = C_o \left(\frac{Q_1 + Q_2}{A} \right) + V_\infty \qquad (30)$$

where Q_1 is the volumetric flow rate of the liquid, i.e., the overflow, OVFL. The average volume concentration $\langle \alpha \rangle$ was assumed to be constant throughout the length of the lifter and the values of C_o and V_∞ were determined as shown in the previous section.

The energies of liquid and gas in a one dimensional steady state flow of an inviscid fluid are given by:

(i) Bernouilli's Equation for a liquid

$$E_1 = \frac{\rho_1 V_1^2}{2} + P + \rho_1 g Z \qquad (31)$$

where ρ_1 is the density of the liquid, V_1 its velocity and P the pressure at some height, Z.

(ii) Saint Venant's Equation for a perfect gas

$$E_2 = \frac{\rho_2 V_2^{\rightarrow 2}}{2} + \rho_2 C_p T + \rho_2 g Z \qquad (32)$$

where ρ_2 is the density of the gas, V_2 its velocity and T the temperature at some height, Z.

Equations (31) and (32) were used to develop energy balances over the length of the 2 phase mixture in the column for two cases as shown in Figure 6.2.1. In case I, the flow rate of gas, Q_2, does not produce any overflow, i.e., $L^* < L^I$. In Case II, the same flow rate, Q_2, produces an overflow.

In these two cases, the flow rate, density and temperature of the gas at the level of the injection nozzle, that is, the bottom of the column is the same. Hence, E_2, given by Equation (32) is the same at the bottom of each lifter:

$$E_2^{I,Bot} = E_2^{II,Bot} \qquad (33)$$

At the top of each lifter, just above the liquid, the velocity of the gas is the same in both cases since the tubes are of equal diameter and the velocity is equal to the average velocity of the gas alone in the column, i.e., Q_2/A. Assuming the pressure and temperature are also the same in both cases at the top, the difference between the energy of the gas above Column I and Column II is obtained form Equation (32):

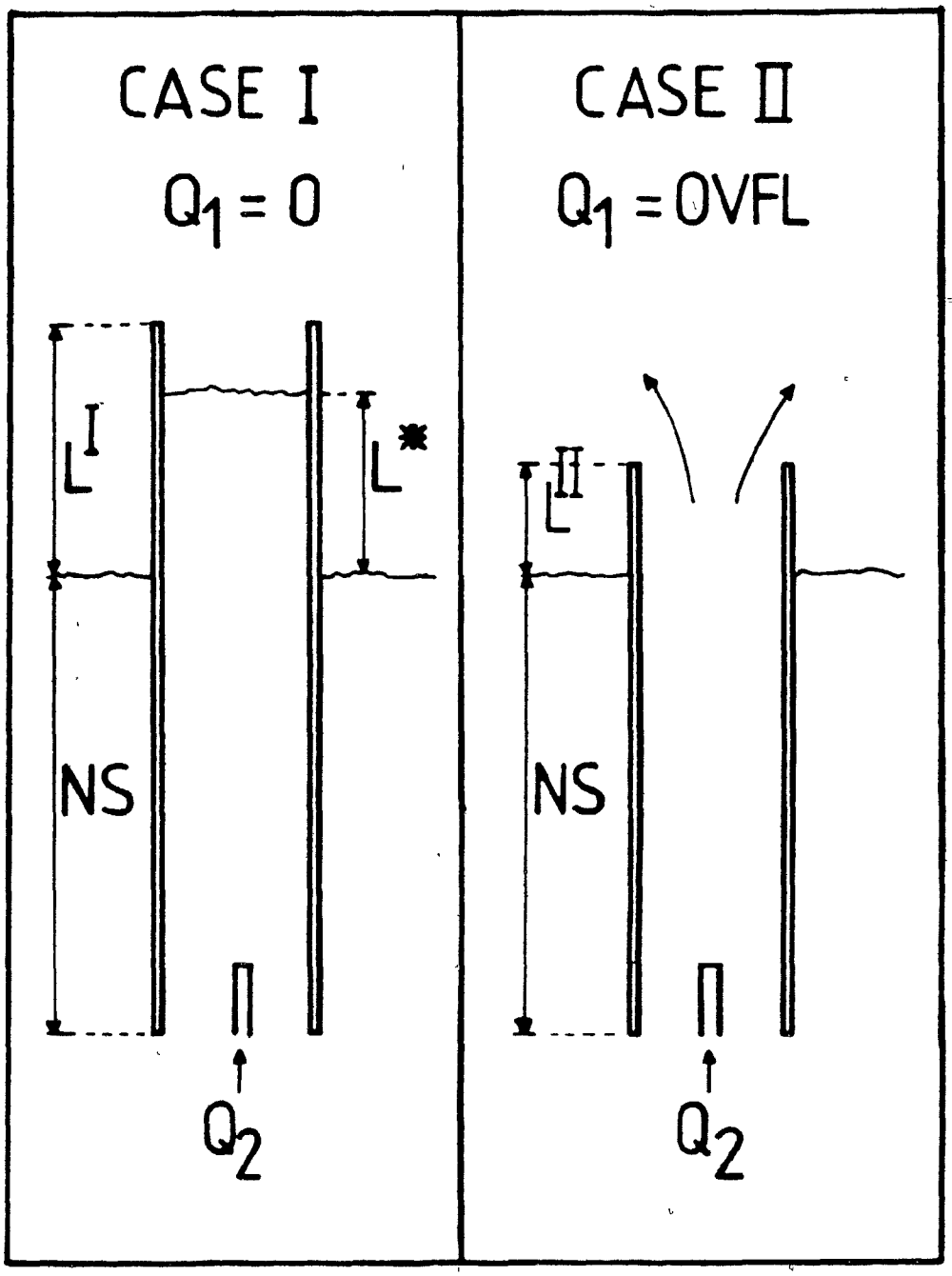

Figure 6.2.1 : The Configurations of the Lift-Spray Systems Considered to Perform Energy Balances.

$$E_2^{I,Top} - E_2^{II,Top} = \rho_2^{Top}.g.\ (L^* - L^{II}) \qquad (34)$$

Now considering the liquid phase, in Case I, there is no liquid entering or leaving the system, hence

$$E_1^{I,Bot} = E_1^{I,Top} = 0 \qquad (35)$$

Now, in Case II, the energy of the liquid entering and leaving the lifter is given by Equation (31) applied at bottom and top respectively. The velocity of the liquid entering and leaving the lifter was assumed to be the same, i.e. void fraction is constant from bottom to top of the lifter.

$$E_1^{II,Bot} - E_1^{II,Top} = \rho_1 g(0 - (L^{II} + NS)) + (P_b - P_T) \qquad (36)$$

P_b and P_T are the pressures at the bottom and top of the column, respectively. However, the pressure at the bottom, P_b, is equal to the top pressure, P_T, plus the hydrostatic pressure, $\rho_1.g.\ (L^{II} + NS)$, i.e.:

$$P_b = P_T + \rho_1.g.\ (L^{II} + NS) \qquad (37)$$

and hence the Equation (36) becomes

$$E_1^{II,Bot} - E_1^{II,Top} = 0 \qquad (38)$$

The difference between the energy accumulated is each system is:

$$E_{ACC}^{I} - E_{ACC}^{II} = \left[(E_1^{I,Bot} + E_2^{I,Bot}) - (E_1^{I,Top} + E_2^{I,Top})\right] - \left[(E_1^{II,Bot} + E_2^{II,Bot}) - (E_1^{II,Top} + E_2^{II,Top})\right] \quad (39)$$

which can be written as:

$$E_{ACC}^{I} - E_{ACC}^{II} = (E_2^{I,Bot} - E_2^{II,Bot}) - (E_2^{I,Top} - E_2^{II,Top}) + (E_1^{I,Bot} - E_1^{I,Top}) - (E_1^{II,Bot} - E_1^{II,Top}) \quad (40)$$

from Equations (33), (35), and (38), the first, third and fourth terms are all equal to zero. Consequently Equation (40) can be written as:

$$E_{ACC}^{I} - E_{ACC}^{II} = - (E_2^{I,Top} - E_2^{II,Top}) \quad (41)$$

This difference is given by Equation (34) and we obtain:

$$E_{ACC}^{I} - E_{ACC}^{II} = \rho_2^{Top}.g.\ (L^{II} - L^{*}) \quad (42)$$

where ρ_2^{TOP} is the density of the gas above the liquid surface. Now, ρ_2^{TOP} is small compared to ρ_1 ($\rho_1 \sim 10^3.\rho_2$) and $(L^{*} - L^{II})$ is not large, therefore

$$E_{ACC}^{I} = E_{ACC}^{II} \tag{43}$$

In other words, the energy accumulated in Column I in the form of potential energy is equal to the energy accumulated in column II in the form of potential and kinetic energies. Again assuming that the density of the gas is negligible compared to the density of the liquid, it is possible to express this in terms of potential and kinetic energies of the liquid:

$$PE^{I} = PE^{II} + KE^{II} \tag{44}$$

From the general laws of mechanics, these can be rewritten as:

$$PE^{I} = \rho_l (1 - \langle \alpha^{I} \rangle).g. \frac{(NS + L^*)}{2} \tag{45}$$

$\rho_l (1 - \langle \alpha I \rangle)$ is the apparent density of Column I, the center of mass is located at a level $(\frac{NS + L^*}{2})$ and the origin is chosen to be the level of the nozzle. Similarly,

$$PE^{II} = \rho_l (1 - \langle \alpha^{II} \rangle).g. \frac{(NS + L^{II})}{2} \tag{46}$$

and, $$KE^{II} = \rho_l \cdot \frac{V_l^2}{2} \tag{47}$$

In these Equations, $\langle \alpha^{I} \rangle$ is given by Equation (27):

$$\langle \alpha^{I} \rangle = \frac{L^*}{L^* + NS}$$

Substituting this in Equation (45):

$$PE^{I} = \rho_l . g . \frac{NS}{2} \qquad (48)$$

Now a combination of Equations (15) and (30) yields:

$$\frac{Q_2}{\langle \alpha^{II} \rangle . A} = C_o . \frac{OVFL + Q_2}{A} + v_\infty \qquad (49)$$

and Equation (49) can be rewritten as:

$$\langle \alpha^{II} \rangle = \frac{Q_2}{C_o . Q_2 - C_o . OVFL + v_\infty . A} \qquad (50)$$

Combining Equations (46), (47), and (48), the energy balance, Equation (44), gives:

$$\rho_l . g . \frac{NS}{2} = \rho_l . \frac{V_l^2}{2} + \rho_l . (1 - \langle \alpha^{II} \rangle) . g . \frac{(NS + L^{II})}{2} \qquad (51)$$

Where $\langle \alpha^{II} \rangle$ is given by Equation (50) and V_l is given by Equation (6), i.e.:

$$V_l = \frac{J_l}{(1 - \langle \alpha^{II} \rangle)} = \frac{OVFL}{A . (1 - \langle \alpha^{II} \rangle)} \qquad (52)$$

Equation (51) can be solved using Equations (50) and (52) to yield an expression for the overflow:

$$OVFL^5.\ (XE^3)$$

$$+\quad OVFL^4.\ (3.XD.XE^2)$$

$$+\quad OVFL^3.\ (3XD^2.XE + gA^2.XE^2.XB)$$

$$+\quad OVFL^2.\ (XD^3 + 2gA^2.XC.XE.XB + gA^2.XE^2.XA)$$

$$+\quad OVFL.\ (gA^2.XC^2.XB + 2gA^2.XC.XE.XA)$$

$$+\quad (gA^2.XC^2.XA)$$

$$= 0 \qquad (53)$$

where $XA = \dot{N}S.Q_2 \cdot \left(\frac{L^{II}}{L^*} - 1\right)$

$XB = C_o.L^{II}$

$XC = (C_o - 1).\ Q_2 + \nu_\infty.A$

$XD = C_o.Q_2 + \nu_\infty.A$

$Xe = C_o$

and L* is given by Equation (29) as:

$$L^* = \frac{Q_2 . NS}{(C_o - 1) . Q_2 + v_\infty . A}$$

6.3. Summary

1. For Lift Experiments, the Lift, L*, inside the lifter tube can be predicted if the distribution parameter, C_o, and the terminal velocity, v_∞, are known.

   L* is given as:

$$L^* = \frac{Q_2 . NS}{(C_o - 1) . Q_2 + v_\infty . A}$$

2. For Lift-Overflow Experiments, the flow rate of liquid, Q_1 or OVFL, can be predicted by solving Equation (53). The solution will be accurate if

   (i) $\rho_2 << \rho_1$

   (ii) $\langle \alpha \rangle$ is constant along the length of the lifter.

CHAPTER SEVEN

DISCUSSION

7.1. Application of the Drift-Flux Model to Lift Experiments and Predictions of Lift

The results of the Lift experiments (Tables 5.1.1. to 5.1.3.) were analyzed with the procedure described in Chapter 6. A number of assumptions with regard to the measurements were made and these are discussed briefly below. The relationship between the weighted mean velocity of the gas and the volumetric flux density of the mixture is then examined.

The gas flow rate as given by the rotameter was corrected to take into account the pressure on the gas line, P_{INJ}, which was different from the pressure used for the calibration of the rotameter, i.e. 76 cm Hg. This correction was made using the "American standard correction factor for variable areas flowmeters" in the case of a gas flow as follows:

$$Q_{2,corr} = Q_{2,meas} \cdot \sqrt{\frac{P_{INJ}}{P_{cal}}} \qquad \text{where } Q_{2,meas} = Q_2'$$

where $Q_{2,corr}$ and $Q_{2,meas}$ are the flow rate corrected and the flow rate read, respectively. P_{INJ} and P_{cal} were the pressure on the gas line and the pressure at which the rotameter was calibrated

respectively,[19]. The volumetric gas flow rate inside the lifting tube, Q_2, was then assumed to be equal to the flow rate calculated at the top pressure, P_{TOP}. Q_2 was therefore given by:

$$Q_2 = Q_{2,corr} \times \frac{P_{cal}}{P_{TOP}}$$

or

$$Q_2 = Q_{2;meas} \times \sqrt{\frac{P_{INJ.} P_{cal}}{P_{TOP}}}$$

The value of the average volumetric flux density of the mixture, $\langle j \rangle$, was then calculated using Equation (25):

$$\langle j \rangle = \frac{Q_2}{A}$$

The weighted mean velocity of the gas, $\bar{V}_2$, was calculated using Equation (28):

$$\bar{V}_2 = \frac{Q_2 (L^* + NS)}{L^* . A}$$

values of $\bar{V}_2$ and $\langle j \rangle$ are listed in Table 7.1.1. for each experiment and $\bar{V}_2$ was plotted as a function of the volumetric flux density of the mixture, $\langle j \rangle$, in Figures 7.1.1. to 7.1.3.

Exp. Number	$\bar{V}_2$	$\langle j \rangle$	Exp. Number	$\bar{V}_2$	$\langle j \rangle$
1-A	36.98	6.49	12-B	41.30	7.70
2-A	50.57	12.64	13-B	28.35	1.13
3-A	29.50	2.95	14-B	30.96	2.38
4-A	40.49	6.85	15-B	36.90	4.10
5-A	58.32	19.91	16-B	37.69	5.95
6-A	38.20	4.93	17-B	28.40	1.14
7-A	31.29	1.65	18-B	29.10	2.24
8-A	45.10	9.80	19-B	38.69	3.65
9-A	50.34	14.57	20-B	38.19	4.86
10-A	27.65	1.47	21-B	30.60	0.62
11-A	37.97	3.80	22-B	32.94	1.32
12-A	38.72	7.04	23-B	34.42	2.02
13-A	43.72	10.93	24-B	35.63	3.36
14-A	34.38	1.23	1-C	28.47	3.16
15-A	32.12	3.21	2-C	49.07	13.38
16-A	35.62	5.09	3-C	67.62	22.54
17-A	42.48	8.24	4-C	74.92	28.22
18-A	46.99	0.85	5-C	26.20	2.02
19-A	30.03	2.07	6-C	43.44	5.53
20-A	34.95	3.50	7-C	43.02	8.02
21-A	38.81	5.01	8-C	64.27	14.11
22-A	37.18	5.81	9-C	21.96	0.88
1-B	71.56	27.52	10-C	33.48	2.58
2-B	27.27	2.57	11-C	37.40	5.34
3-B	47.84	8.25	12-C	37.81	7.56
4-B	60.54	15.83	13-C	24.52	0.74
5-B	67.47	23.71	14-C	32.12	1.89
6-B	30.42	1.51	15-C	36.50	3.44
7-B	38.64	4.29	16-C	38.52	4.90
8-B	49.48	8.53	17-C	27.86	2.39
9-B	52.31	11.81	18-C	34.19	3.80
10-B	26.10	1.54	19-C	28.75	1.15
11-B	38.51	2.96	20-C	30.62	2.08

Table 7.1.1. Values of the Weighted Mean Velocity V_2, and the Average Flux Density of the Mixture, $\langle j \rangle$.

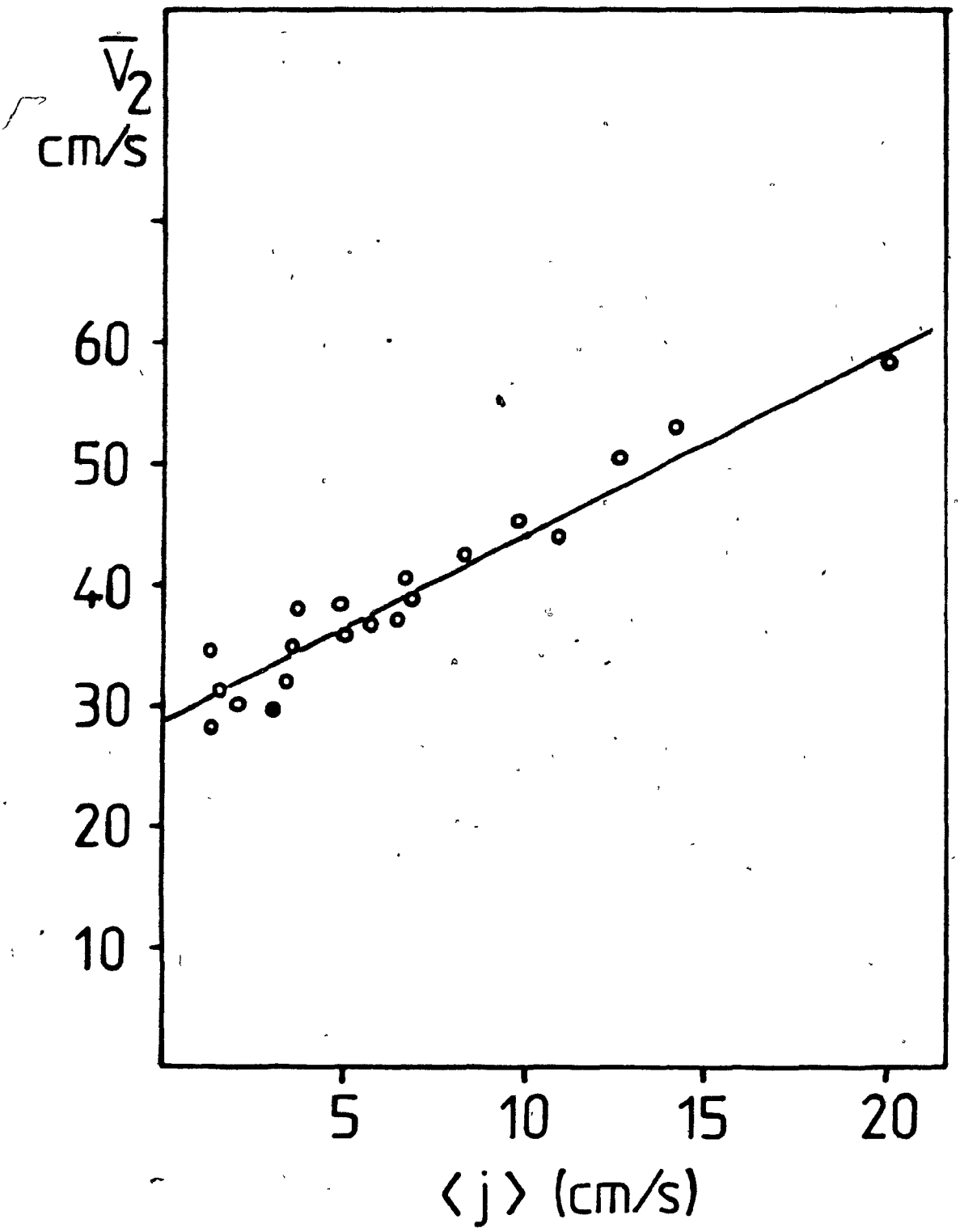

Figure 7.1.1 : Weighted Mean Velocity of the Gas vs. Volumetric Flux Density of the Mixture for the 3" O.D. Lifter.

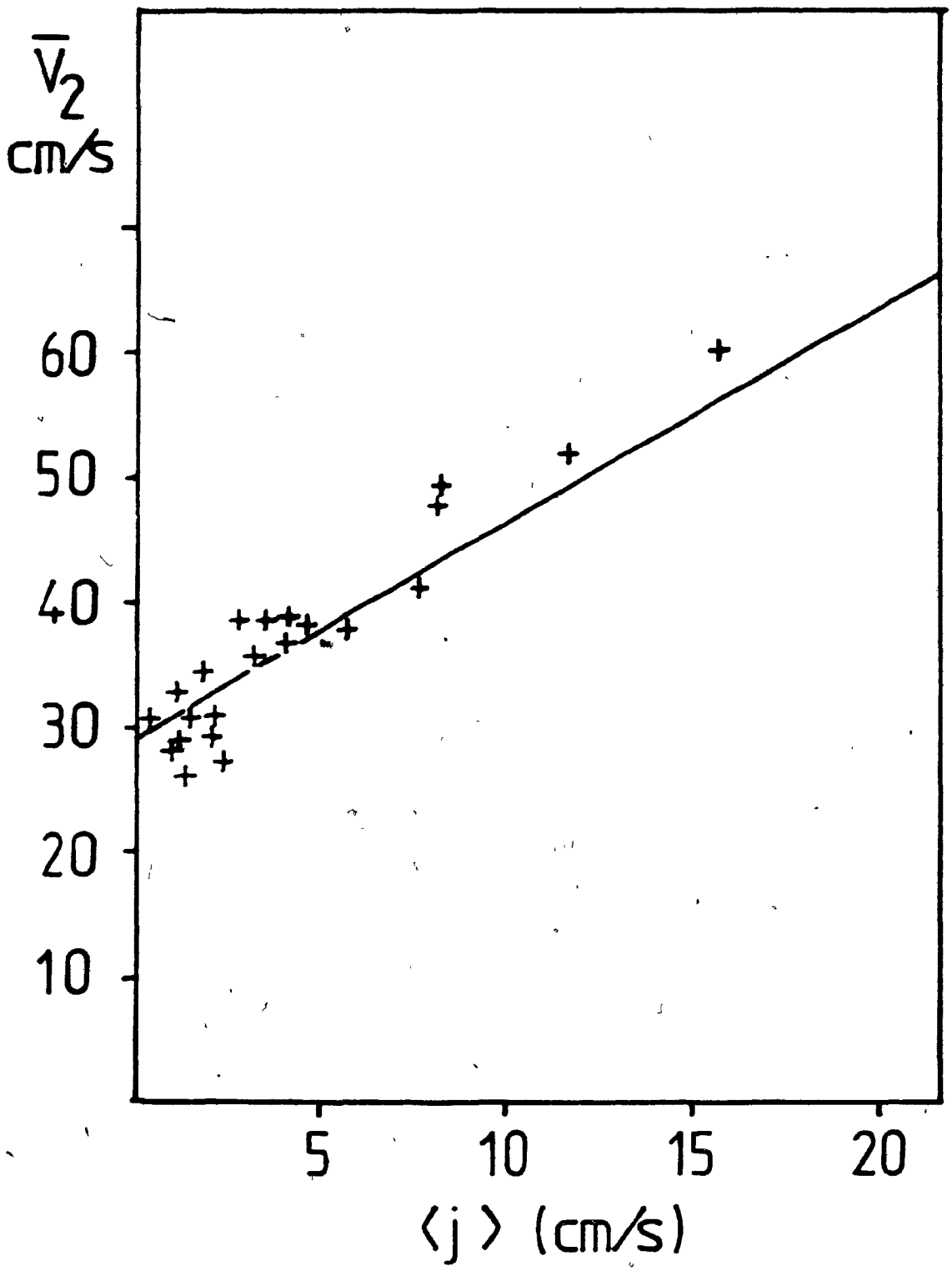

Figure 7.1.2 : Weighted Mean Velocity of the Gas vs. Volumetric Flux Density of the Mixture for the 4" O.D. Lifter.

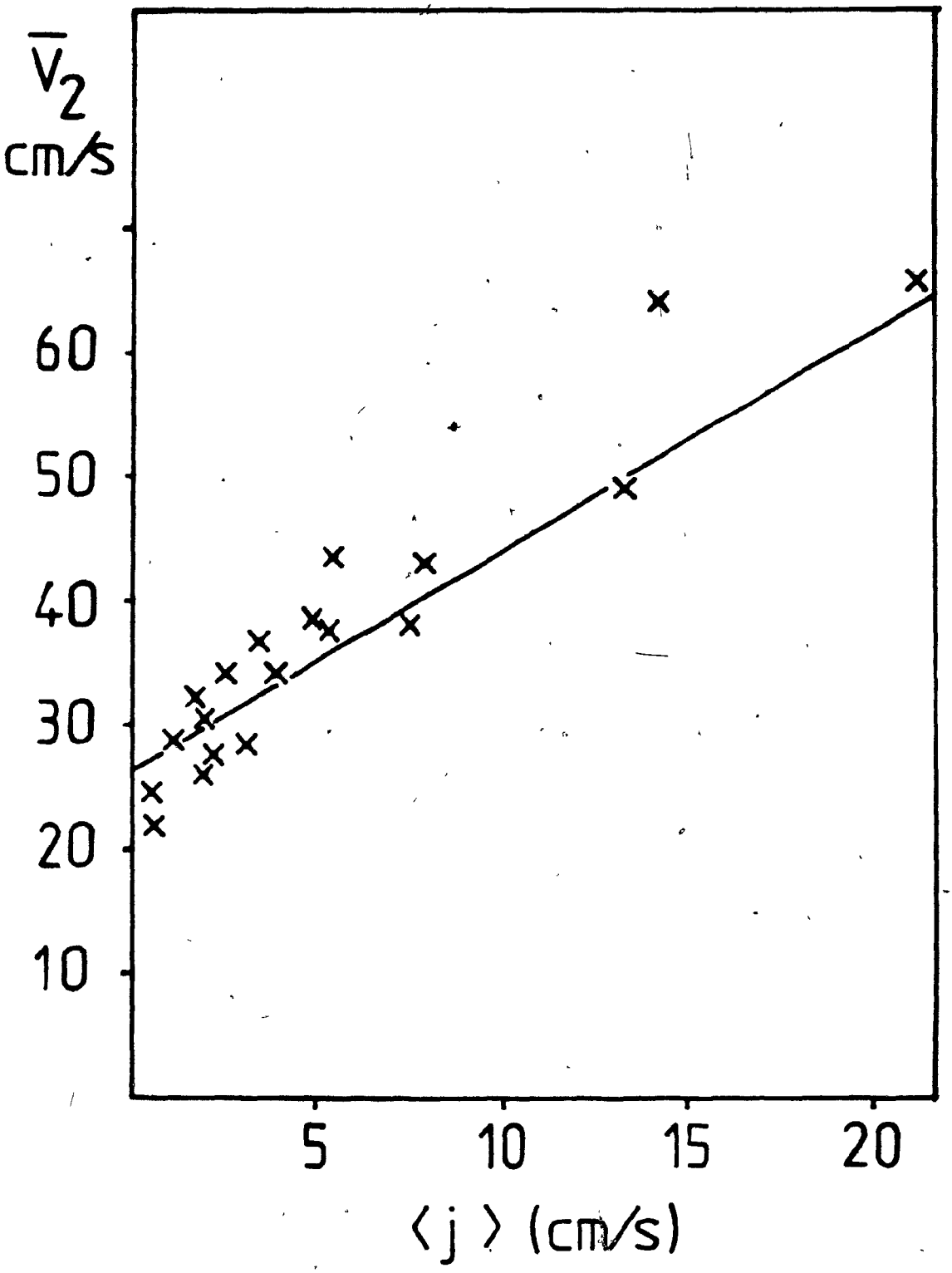

Figure 7.1.3 : Weighted Mean Velocity of the Gas vs. Volumetric Flux Density of the Mixture for the 5" O.D. Lifter.

The linearity of these curves is obvious and confirmed by linear regressions performed on the data which gave the following results.

for 3" Tube $\bar{V}_2 = 1.54 \langle j \rangle + 28.75$ (correlation 96.2%)

for 4" Tube $\bar{V}_2 = 1.71 \langle j \rangle + 29.10$ (correlation 96.3%)

for 5" Tube $\bar{V}_2 = 1.79 \langle j \rangle + 26.42$ (correlation 97.2%)

A linear regression for all date (see Fig. 7.1.4) gave

$\bar{V}_2 = 1.71 \langle j \rangle + 27.98$ (correlation 96.2%)

Experiment (18-A) was not used in the computation of the regression line. For this point, the value of L* is small and is believed to be erroneous. Experiment (8-C) was not consider either, since the value of the top pressure was uncertain.

The value of the distribution parameter, C_o, which is the slope of the line in Figures 7.1.1. to 7.1.3. indicates that the volume concentration, α, and the gas velocity, V_2, are both higher in the center of the lifter than on the wall. The increasing value of C_o for increasing diameter of lifter suggest that higher volume concentration and gas velocity in the center are favored with larger lifting tubes as compared to the smaller tubes.

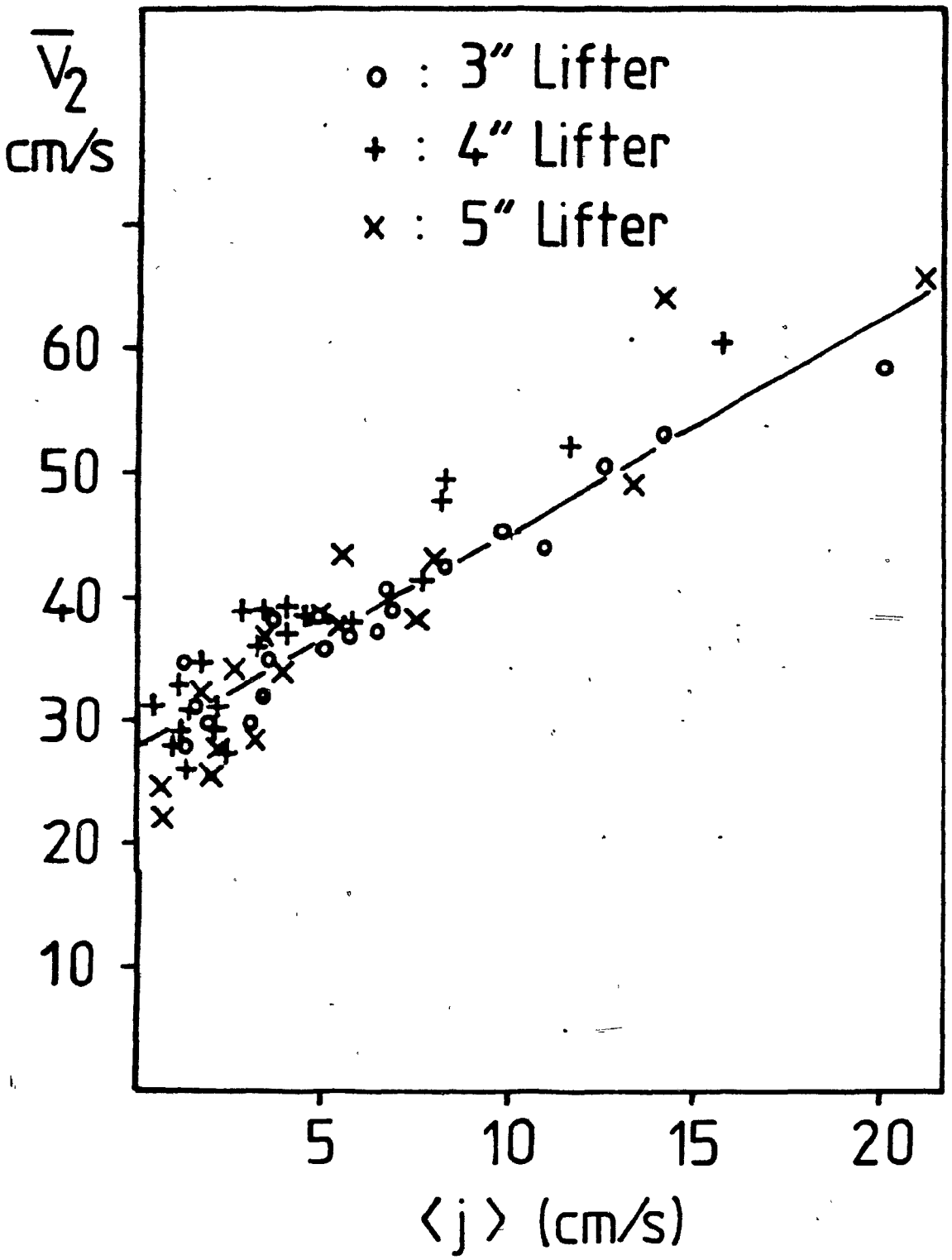

Figure 7.1.4 : Weighted Mean Velocity of the Gas vs. Volumetric Flux Density of the Mixture for the 3", 4", and 5" O.D. Lifter.

Theoretical values of the terminal velocity, v_∞, are given in Table 7.1.2. for the churn-turbulent bubbly flow and the slug flow regime using Equations (22) and (23). The value of the surface tension is taken from the Handbook of Chemistry and Physics [20] and is estimated to be 73 dynes/cm for a Nitrogen-Water system. The calculated values of the intercept are also shown in Table 7.1.2. These are not seen to increase with an increase in the diameter of the lifter and, therefore, conforms with the fact that only a churn turbulent flow regime was observed.

With the above correlations for C_o and v_∞, it was possible to make theoretical predictions of the Lift, L*, in the system using Equation (29). The values of C_o and v_∞ which were used were those obtained regression of $\bar{V}_2$ vs. $\langle j \rangle$ for all data, i.e., 3", 4", and 5" tubes. These predictions are listed in Tables 7.1.3. to 7.1.5. The agreement with the experimental values is excellent. Consequently, the values of $C_o = 1.71$ and $v_\infty = 28.0$ were assumed to be accurate enough to describe the two-phase flow for any tube diameter.

7.2. Application of the Energy Balance to Overflow Experiments. Predictions of Overflow

The results of the Overflow Experiments (Table 5.2.1.) were analyzed and compared to the predictions made using the procedure described in Chapter 6. Again, the gas flow rate given by the direct

Lifter Diameter	Churn-Turbulent bubbly flow	Slug flow	Experimental Value (from plot)
6.8 cm	25.02 cm/s	28.58 cm/s	28.75 cm/s
9.3 cm	25.02 cm/s	33.43 cm/s	29.10 cm/s
12.0 cm	25.02 cm/s	37.97 cm/s	26.42 cm/s

Table 7.1.2. Comparison between the values of the terminal velocities obtained from the experimental data and the predicted values for churn-turbulent bubbly flow (Equation 22), and slug flow regime (Equation 23).

Experiment Number	$\overline{L^*}$ Experimental	L^* Computed
1-A	11.5	10.75
2-A	18.0	18.46
3-A	6.0	5.29
4-A	11.0	11.26
5-A	28.0	25.52
6-A	8.0	8.45
7-A	3.0	3.05
8-A	15.0	15.14
9-A	22.0	20.52
10-A	3.0	2.71
11-A	6.0	6.68
12-A	12.0	11.52
13-A	18.0	16.50
14-A	2.0	2.30
15-A	6.0	5.73
16-A	9.0	8.69
17-A	13.0	13.15
18-A	1.0	1.61
19-A	4.0	3.80
20-A	6.0	6.21
21-A	8.0	8.57
22-A	10.0	9.76

Table 7.1.3. Comparison Between Experimental Data and Predictions Obtained With

$C_o = 1.71$ and $\nu_\infty = 28.00$

for Lift in a 3" Tube (6.8 cm I.D.)

Experiment Number	L* Experimental	L* Computed
1-B	30.0	27.79
2-B	5.0	4.14
3-B	10.0	11.69
4-B	17.0	19.37
5-B	26.0	25.38
6-B	2.5	2.49
7-B	6.0	6.64
8-B	10.0	12.02
9-B	14.0	15.58
10-B	3.0	2.53
11-B	4.0	4.72
12-B	11.0	11.04
13-B	2.0	1.89
14-B	4.0	3.85
15-B	6.0	6.37
16-B	9.0	8.86
17-B	2.0	1.89
18-B	4.0	3.63
19-B	5.0	5.73
20-B	7.0	7.42
21-B	1.0	1.05
22-B	2.0	2.19
23-B	3.0	3.30
24-B	5.0	5.31

Table 7.1.4. Comparison Between Experimental Data and Predictions Obtained With

C_o = 1.71 and v_∞ = 28.00

for Lift in a 4" Tube (9.3 cm I.D.)

Experiment Number	L* Experimental	L* Computed
1-C	6.0	5.02
2-C	18.0	17.13
3-C	24.0	24.59
4-C	29.0	28.20
5-C	4.0	3.29
6-C	7.0	8.31
7-C	11.0	11.43
8-C	13.5	17.81
9-C	2.0	1.47
10-C	4.0	4.14
11-C	8.0	8.07
12-C	12.0	10.88
13-C	1.5	1.25
14-C	3.0	3.09
15-C	5.0	5.43
16-C	7.0	7.47
17-C	4.5	3.86
18-C	6.0	5.94
19-C	2.0	1.92
20-C	3.5	3.39

Table 7.1.5. Comparison Between Experimental Data and Predictions Obtained With $C_o = 1.71$ and $\nu_\infty = 28.00$ for Lift in a 5" Tube (12.0 cm I.D.)

reading of the rotameter, $Q_{2,meas}$ was corrected to take into account the pressure on the gas line, P_{INJ}.

A theoretical value of the overflow was calculated using the Fortran Program listed in Appendix I which solves equation (49). The computed values of the overflow are listed in Table 7.2.1 together with the experimental values. Figure 7.2.1 is a plot of the overflow computed as a function of the overflow measured. This graph shows that:

(i) The results of the prediction are in good agreement with the experimental data.

(ii) In general, the predicted values are larger than the experimental values. This is probably due to leakage from the top section of the tank to the bottom one. (see Figure 3.3.1.).

(iii) The values obtained using the submersible pump are bad when compared to the predicted values. This tends to prove that this method of measurements was not accurate enough to make good measurements of the overflow.

7.3. Other Considerations Pertaining to the Computations

7.3.1. Lift Experiments

In Section 6.1, a number of simplifying assumptions were made in order to apply the drift-flux model to the system. These are discussed below:

Experiment Number	OVFL Measured	OVFL Computed
1-D	72	0
2-D	1570	1590
3-D	1064	1045
4-D	174	485
5-D	561	756
6-D	424	650
7-D	455	458
8-D	314	536
9-D	62	349
10-D	490	615
11-D	424	704
12-D	200 *	609
13-D	138 *	429
14-D	176 *	745
15-D	143 *	383
16-D	103 *	526
17-D	179 *	572
18-D	147 *	494
19-D	2690	2837
20-D	1962	2225
21-D	3139	2509
22-D	1189	1863
23-D	1054	1718
24-D	1347	1766
25-D	2092	2011
26-D	1327	1606
27-D	975	1524
28-D	1171	1636
29-D	1635	1766
30-D	1046	1167
31-D	923	1200
32-D	1021	1215

Table 7.2.1. Comparison Between Measured Overflow and Computed Overflow.

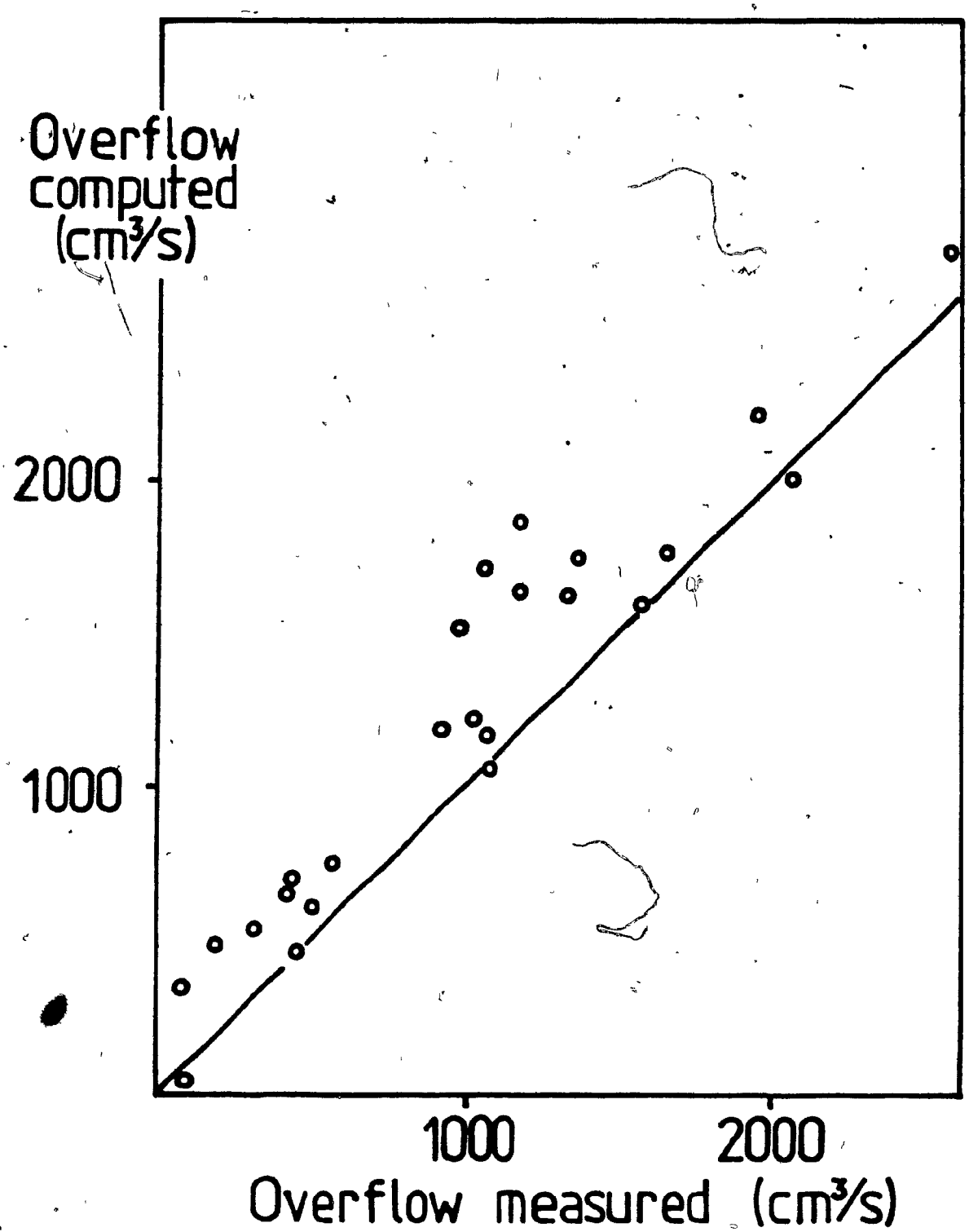

Figure 7.2.1 : Computed Overflow vs. Measured Overflow

(the line is the ideal case)

(i) $\langle\alpha\rangle$ was constant over the length of the lifter

This assumption enabled the determination of $\langle\alpha\rangle$ from the experimental value of L* using Equation (27). This condition may only apply for a lifter of reasonable dimensions in which the variation of total pressure from the nozzle to the top of the two-phase region is not too large.

(ii) Q_2 was constant over the length of the lifter

The same limitations as for $\langle\alpha\rangle$ are likely. However, in most cases, the pressure drop in the column was usually a fraction of the top pressure. Therefore, the top pressure was assumed to be a good approximation of the pressure required to calculate the volumetric flow rate of gas. In other cases, this assumption simplified the calculations. Since the results seemed in good agreement with the predictions, no other assumptions were considered. However, correction could have to be done when using more dense fluids.

7.3.2. Overflow Experiments

In Section 6.2, the simplyfing assumptions which were made in the application of the drift-flux model to the Lift experiments and discussed in the previous section, were used again. Provided that these assumptions are again valid, the predictions of the overflow rate can be made as shown in Section 6.2., since the model is based on

the fact that a system with no overflow and a similar system with overflow have accumulated the same amount of energy (Equation 43).

7.4. General Prediction of the Model Showing the Influences of Operational Parameters

7.4.1. Influence of Lifter Diameter, D.

The computed effect of the lifter diameter on overflow is shown in Figures 7.4.1. to 7.4.3. for various gas flow rates, Q_2, and Lifter Heights, L. The Nozzle Submergence, NS, was kept constant, i.e. NS = 100 cm.

When the area of the lifter decreases to small values, the gas floods the lifter and no liquid overflow occurs. On the other hand, when the lifter cross-sectional area increases to very large values, the potential lift becomes less than the Lifter Height and therefore, no liquid overflow occurs. Consequently, a maximum value of the overflow exists for a particular value of the area, A^{max}.

Considering the plot of $\bar{V}_2$ versus $\langle j \rangle$ (Fig. 7.1.4.), this can be interpreted as follows:

(i) If $A < A^{max}$, the product $\langle \alpha \rangle A'$ must increase as A increases with constant gas flow rate, Q_2

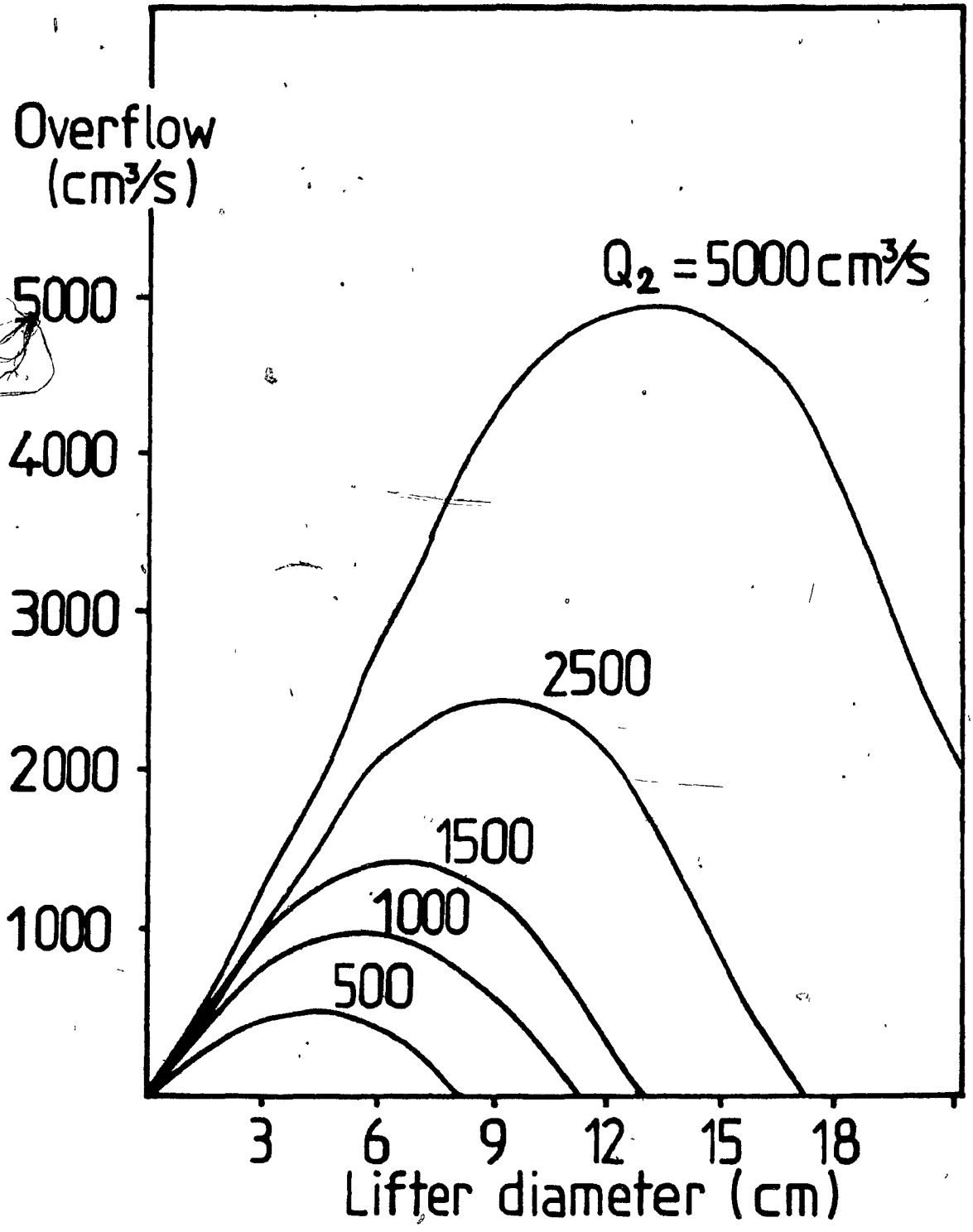

Figure 7.4.1 : Overflow Rate vs. Lifter Diameter for Various Injection Flow Rates. (L = 30 cm ; NS = 100 cm)

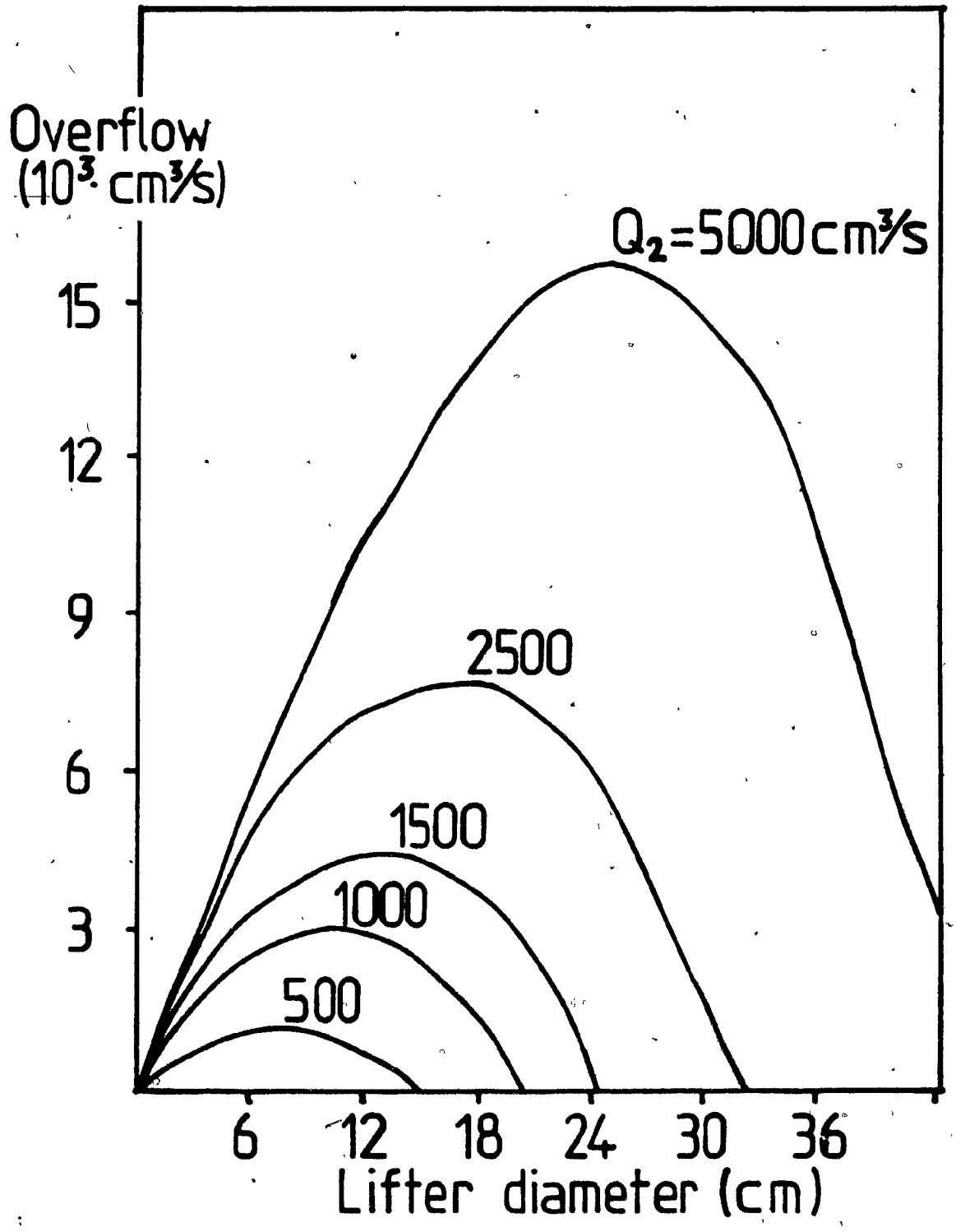

Figure 7.4.2 : Overflow Rate vs. Lifter Diameter for Various Injection Flow Rates. (L = 10 cm ; NS = 100 cm)

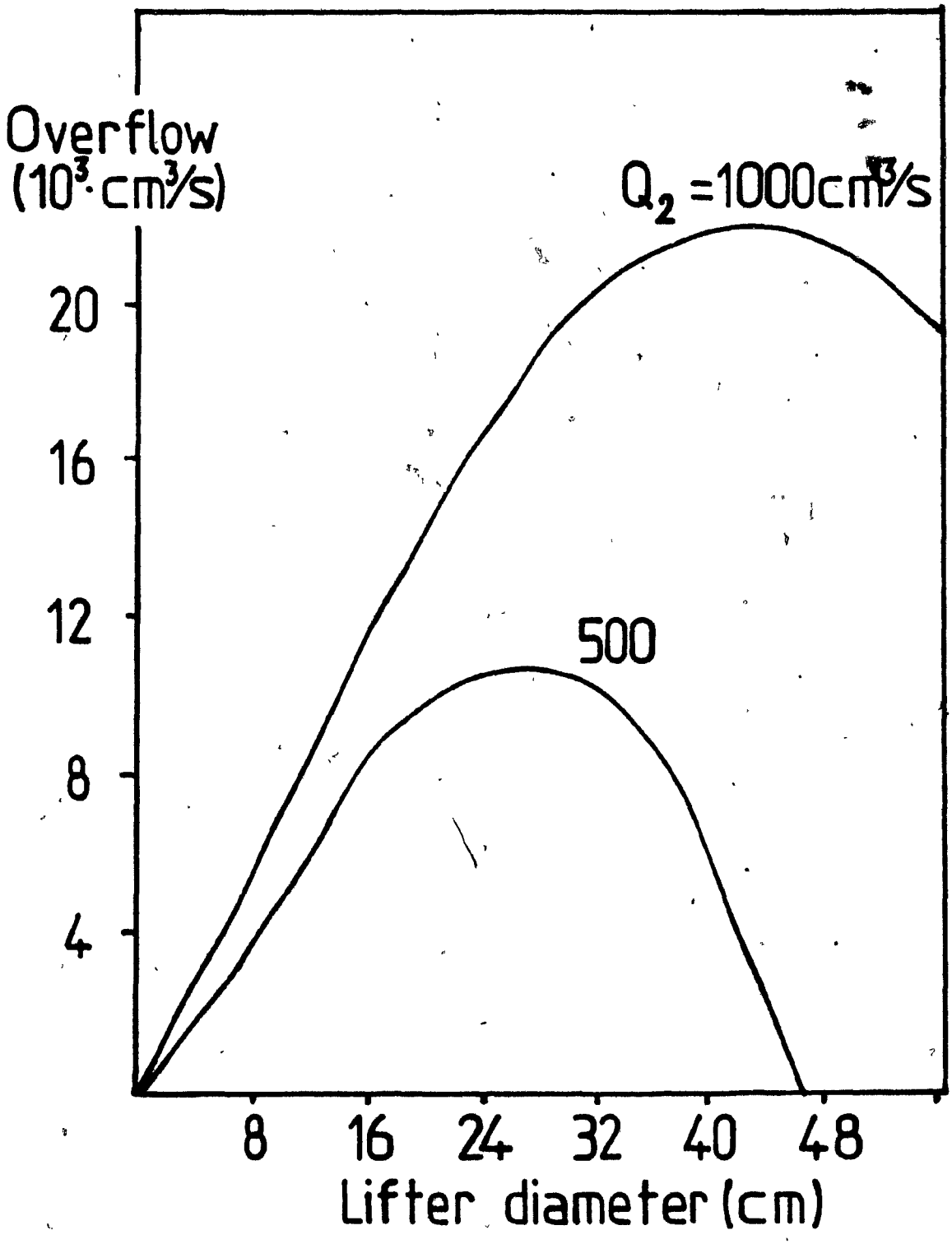

Figure 7.4.3 : Overflow Rate vs. Lifter Diameter for Various Injection Flow Rates. (L = 1 cm ; NS = 100 cm)

(ii) if $A > A^{max}$, the product $\langle\alpha\rangle A$ must decrease as A increases with constant gas flow rate, Q_2

Due to the complexity of Equation (53), it was not possible to obtain an analytical expression for the value of A^{max}. However, Figure 7.4.4. is a nomograph giving this optimum value when the flow rate, the Nozzle Submergence and the Lifter Height are as shown.

Figures 7.4.1. to 7.4.3. also show that the higher the gas flow rate, the higher the overflow. As well, they show that the higher the Lifter Height the lower the overflow. This will be discussed more specifically in the following sections.

7.4.2. Influence of Lifter Height, L.

Figure 7.4.5. shows the effect of Lifter Height, L, on the overflow for various Nozzle Submergences, flow rate and diameter being held constant, i.e.: $D = 10$ cm

$Q_2 = 1000$ cm^3/s

These curves confirm the fact that the higher the Lifter Height, L, the lower the overflow will be; when L eventually reaches the value of the potential lift L*, the overflow becomes equal to zero.

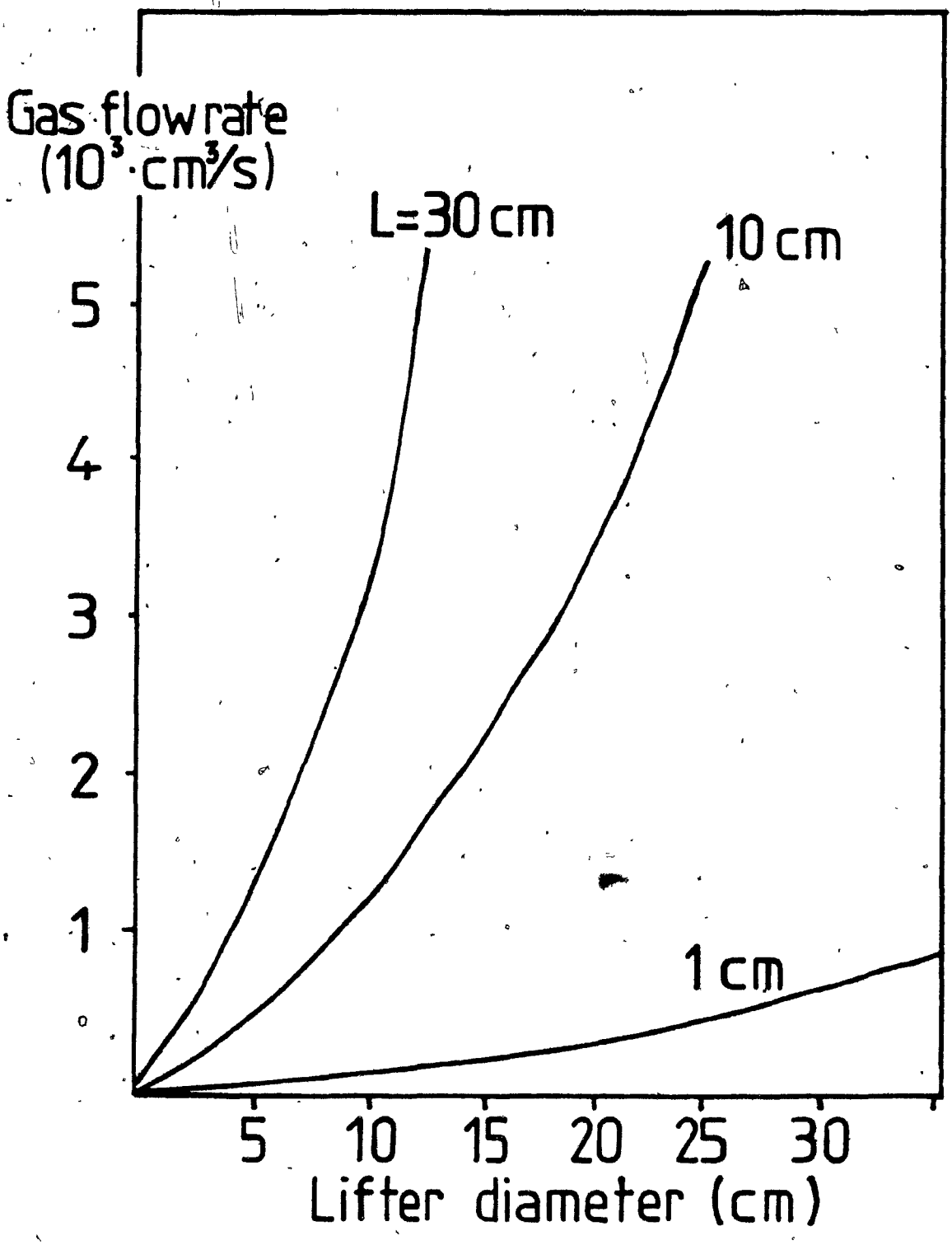

Figure 7.4.4 : Injection Flow Rate Required to Optimize the Overflow Rate in Terms of Lifter Diameter. (NS = 100 cm)

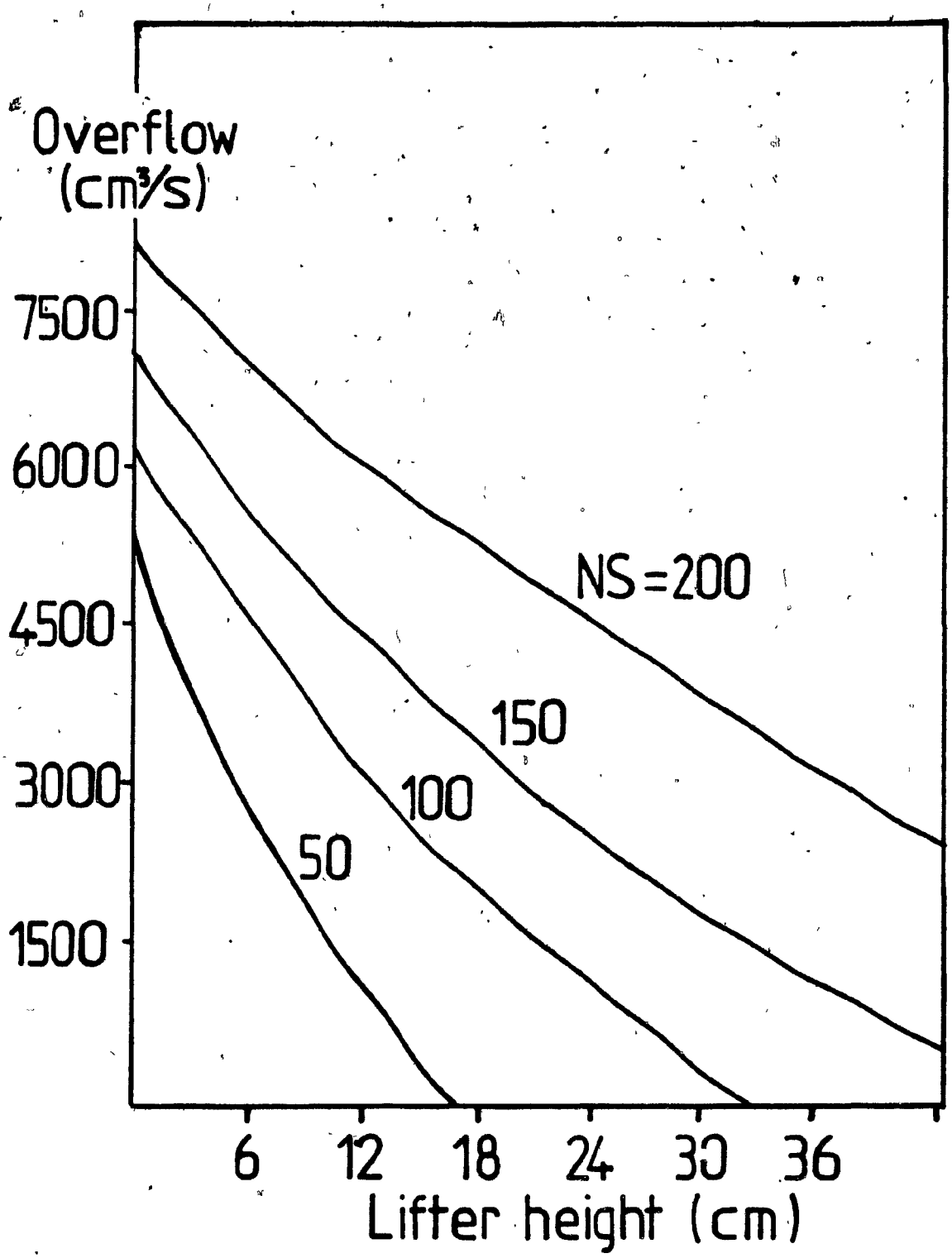

Figure 7.4.5 : Overflow Rate vs. Lifter Height for Various Values of the Nozzle Submergence. (D = 10 cm ; Q_2 = 1000 cm^3/s)

7.4.3. Influence of Nozzle Submergence, NS

Figure 7.4.6 shows the effect of Nozzle Submergence on the overflow; diameter, height of lifter and flow rate remaining constant. These were chosen arbitrarily to be:

$D = 10$ cm

$L = 10$ cm

$Q_2 = 1000$ cm^3/s

This curve shows that when the nozzle submergence increases, the overflow remains zero as long as L* is less than L, then it starts to increase as the fifth root of the nozzle submergence, i.e.,

$$OVFL \sim NS^{1/5} \qquad \text{(see Equation 53).}$$

7.4.4. Influence of Gas Injection Flow Rate; Q_2.

Figure 7.4.7 represents the variation of the overflow as a function of gas flow rate for a given diameter, Lifter Height and Nozzle Submergence. This curve has a similar appearance to the previous one, with overflow only when L* > L and increasing overflow with an increase in the flow rate. However, looking at Equation (29) and allowing Q_2 to tend to infinite values, the coefficients which also tend to infinity are:

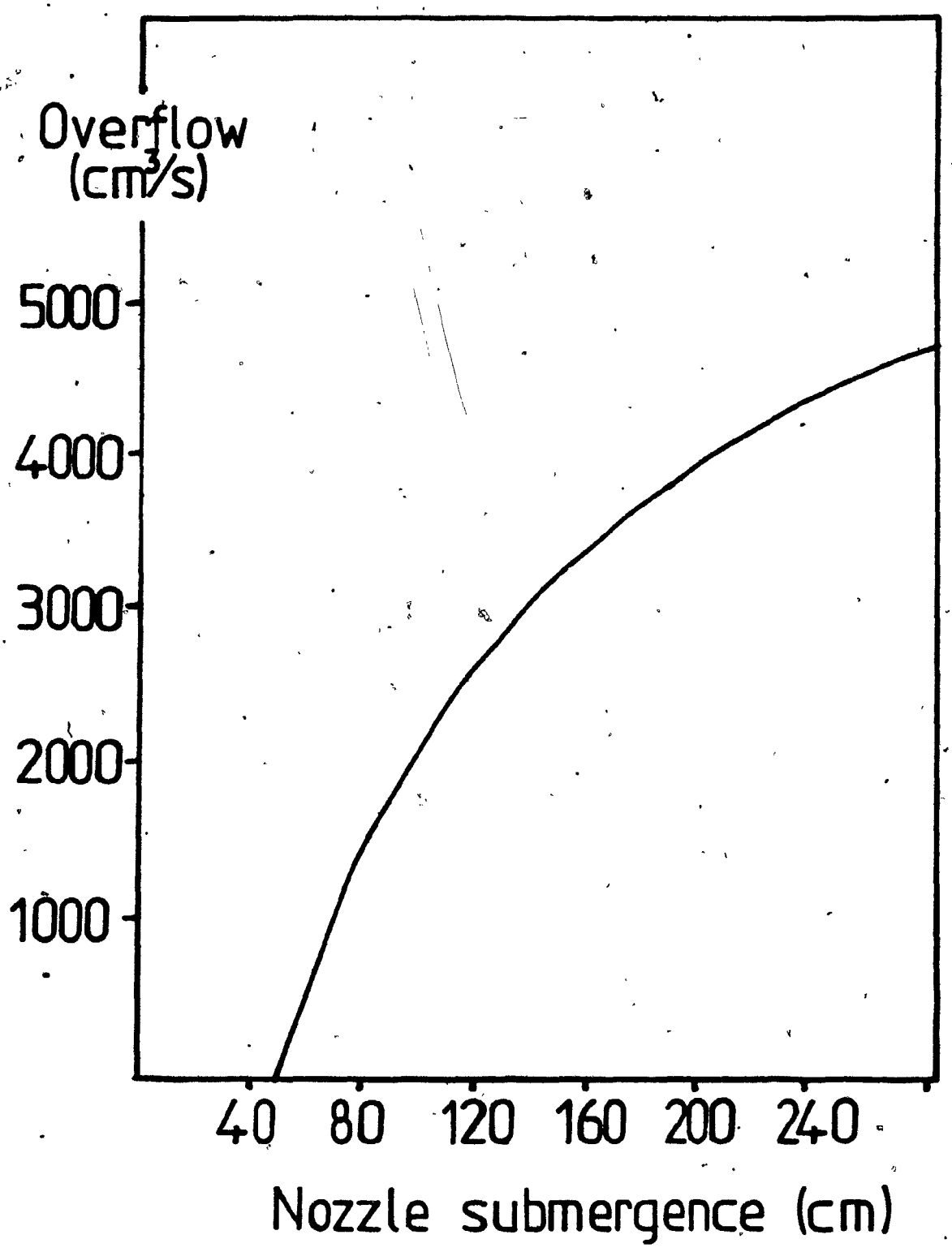

Figure 7.4.6: Overflow Rate vs. Nozzle Submergence

(D = 10 cm ; L = 10 cm ; Q_2 = 1000 cm^3/s)

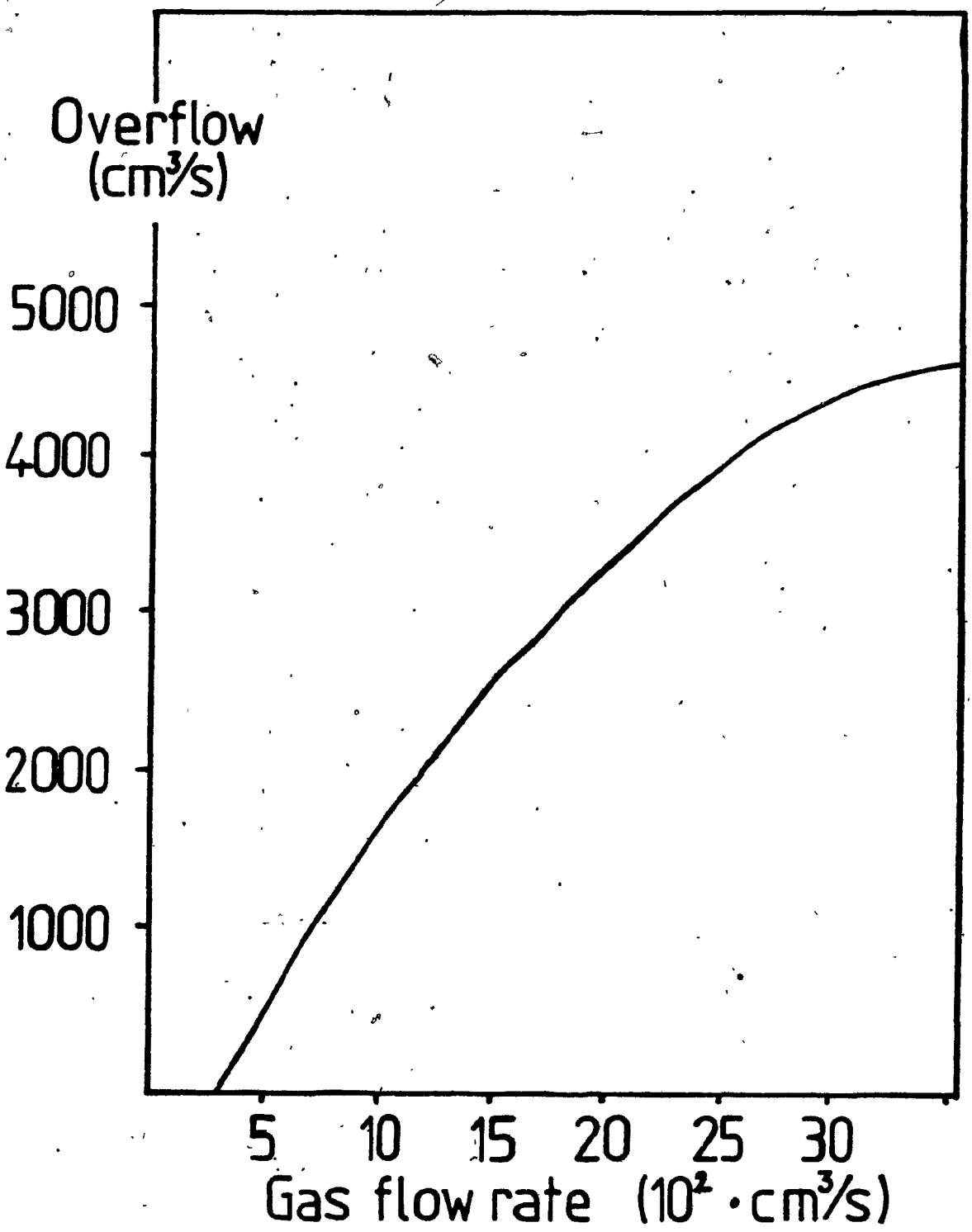

Figure 7.4.7 : Overflow Rate vs. Gas Injection Flow Rate

(D = 10 cm ; L = 10 cm ; NS = 100 cm)

$$XA \longrightarrow NS \cdot Q_2 \left(\frac{L}{NS} \cdot (C_o - 1) - 1 \right)$$

$$XC \longrightarrow (C_o - 1) \cdot Q_2$$

$$XD \longrightarrow C_o \cdot Q_2$$

therefore Equation (29) becomes, in this limiting case:

$$OVFL^2 \ (XD^3) + (gA^2 . XC^2 . XA) = 0 \qquad (54)$$

in which only the higher degree terms have been kept. It is seen from Equation (54) that the overflow reaches a limiting value given by:

$$OVFL = \sqrt{g} A . \frac{XC}{XD} \sqrt{\frac{-XA}{XD}}$$

or, expanding the coefficents:

$$OVFL = \sqrt{g} . A . \frac{(C_o - 1)}{C_o} \sqrt{-\frac{NS}{C_o} \ \frac{L}{NS} . (C_o - 1) - 1}$$

Furthermore, the maximum value of the overflow is obtained when the Lifter Height, L, is equal to zero, i.e.

$$OVFL = gA \frac{(C_o - 1)}{C_o} \sqrt{\frac{NS}{C_o}} \qquad (55)$$

Since the Lifter Height is usually much less than the Nozzle Submergence, the expression above can be used as a good approximation of the overflow which can be achieved in any system whose dimensions (i.e. NS, L, and D) are known.

7.4.5. Effect of Vacuum

As shown in the previous section, the important parameter for high circulation rates is the volumetric flow rate of gas and not the molar flow rate. Hence, the application of vacuum to a system with a given molar flux will increase the volumetric flow rate. Consequently, under low pressures, the lift and overflow rates are enhanced for a given molar gas flow rate.

7.5. Comparison with Previous Studies

The results of the Kobe Steel GMR process [15], were compared to the theoretical predictions of our model. The water model used by Kobe Steel was a 700 tons water tank with lifter sizes from 30 cm to 70 cm internal diameter. The Nozzle Submergence was kept constant at 220 cm and the flow rate was varied up to 25 m^3/ min. The results of the measurements made by Kobe Steel are shown in Figure 7.5.1. Figure 7.5.2. shows our predictions in which the Lifter Height was corrected to take into account the fact that the lifter tube in the GMR process is bent horizontal at the top opening. The predictions of the model are in very good agreement with the experimental results obtained in

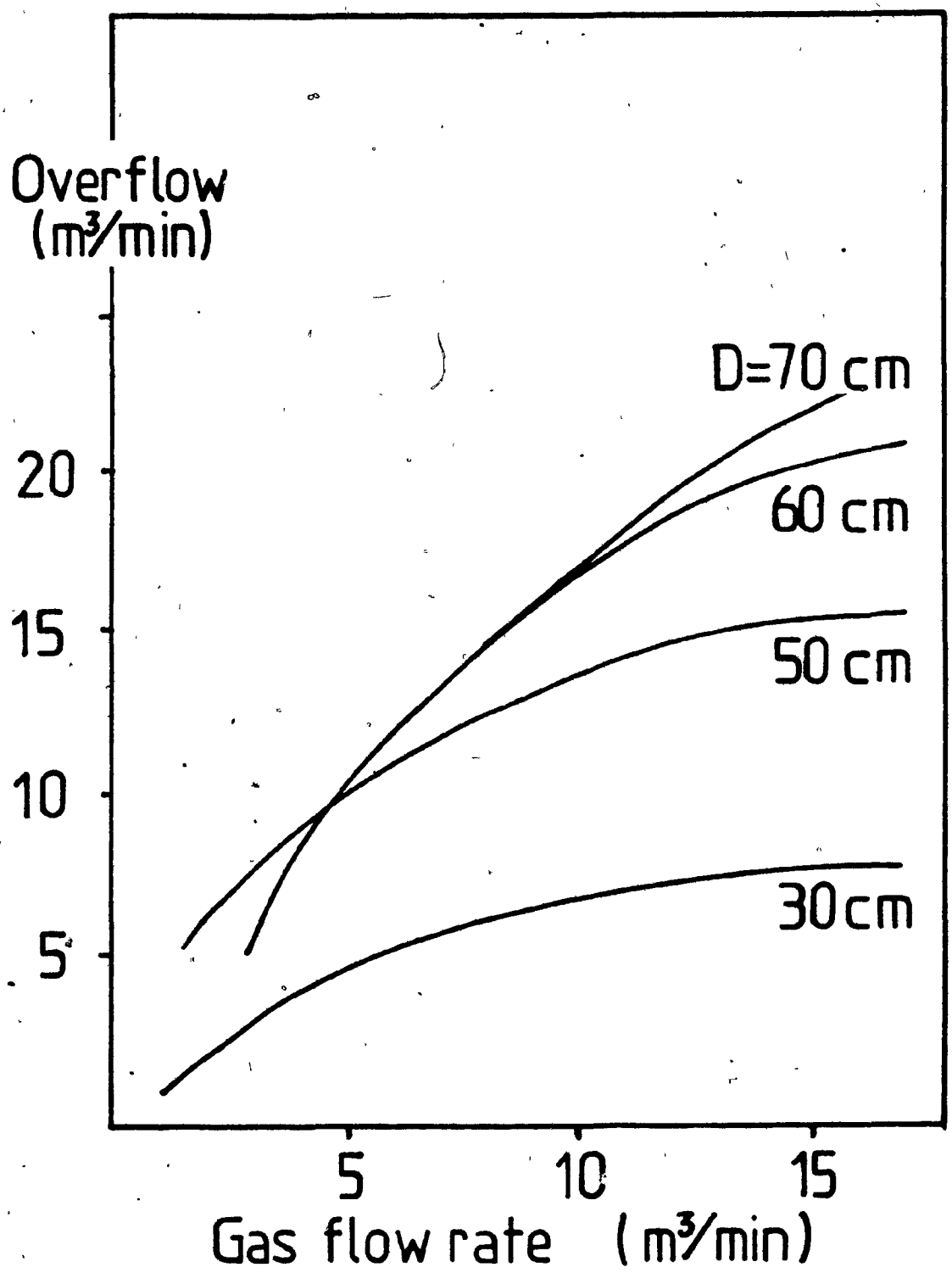

Figure 7.5.1 : Overflow vs. Gas Flow Rate in the G.M.R. Process.

Experimental Data obtained on Water at Kobe Steel.

(L = 20 cm ; NS = 220 cm)

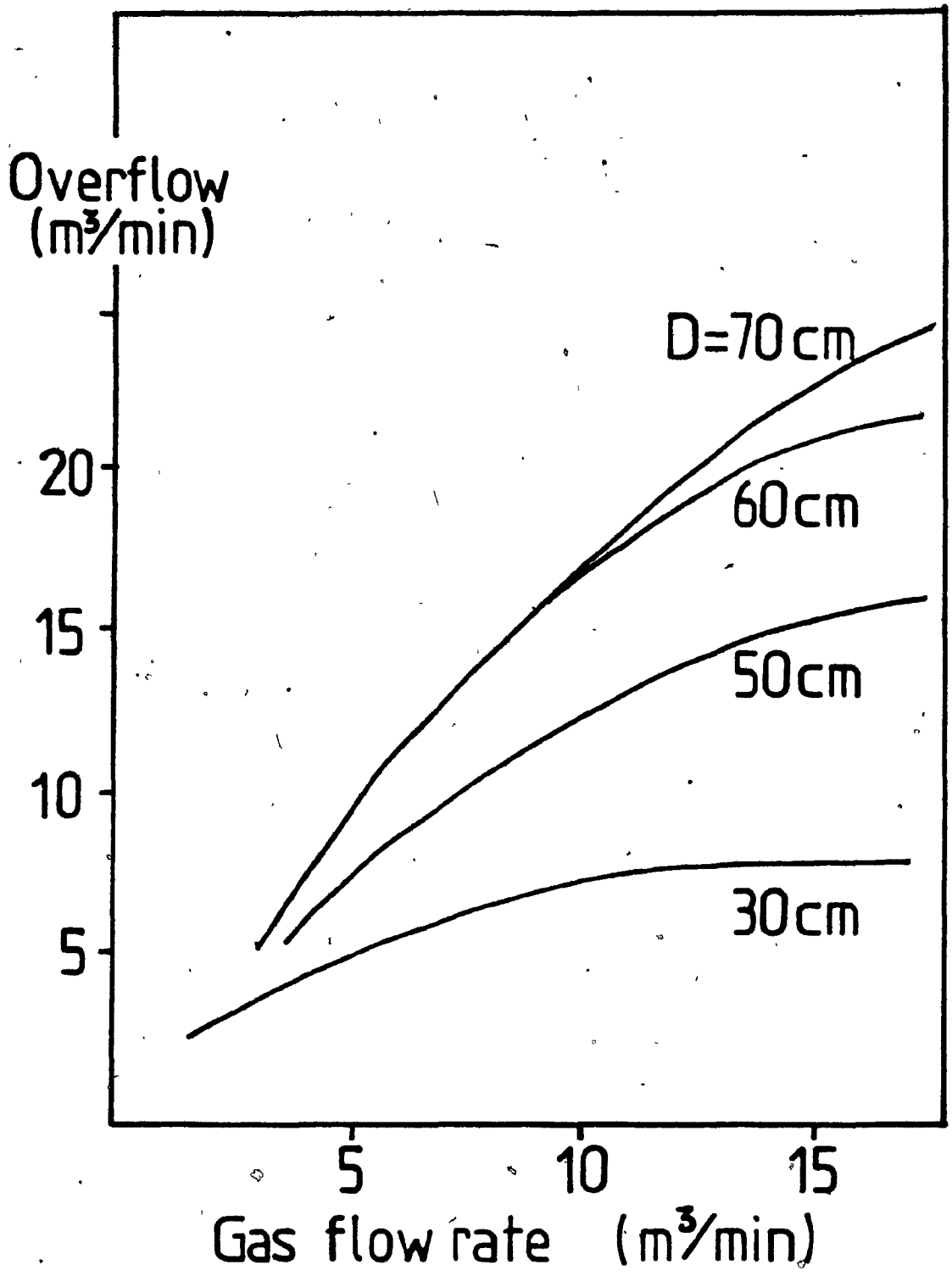

Figure 7.5.2 : Overflow vs. Gas Flow Rate as Predicted by the Model, Using the Dimensions of the G.M.R. System, ($C_o = 1.6$)

the GMR model since these results were obtained with operational parameters far apart from ours and alludes to the wide range of application of the model.

7.6. Extrapolation to Liquid Metals

It can be seen that, in the final expression for liquid overflow rates, (Equation 53), the density of the liquid, ρ_l, is no longer a parameter. Therefore the model is most likely applicable to the circulation rates for liquid metals in gas-lift pumps, with the proviso that the simplifying assumptions remain valid.

The results obtained at Kobe Steel in the GMR process indicated that the circulation flow rate of molten pig iron was almost equal to that of water. It is also reported in the literature that the circulation flow rate in RH degassing apparatus is 20t/min for an apparatus having a capacity of 60 to 100t or 40t/min for an apparatus having a capacity of 150 to 200t. Further in ASEA-SKF furnaces of 100t the circulation flow rate is 70 to 85t/min. It is rather difficult to compare these values directly with the results of the model, but these circulation rates are of the same order of magnitude as those obtained with the model.

CHAPTER EIGHT

CONCLUSIONS

The conclusions drawn from the thesis were:

(1) Photographic observation has shown that in a two-phase flow system, low pressures favour churn-turbulent bubbly flows.

(2) Experiments were carried out showing that a maximum potential lift exists for any set of conditions, i.e. NS, D, Q_2.

(3) Experiments showed that when $L_s < L^*$ overflow occured.

(4) Such flows can be described by the drift-flux model, which takes into account the effect on non-uniform flow and concentration profiles, and considers the relative velocity between the phases.

(5) The drift-flux model accurately predicts the potential lift in a lifting tube using the gas flow rate, top pressure and nozzle submergence.

(6) A theoretical model based on the principle of conservation of energy and on the drift flux model was developed to predict the overflow rate in a Lift-Spray system.

(7) The overflow rate was found to be the solution of a five degree equation which can be expressed in terms of gas flow rate, top pressure, Nozzle Submergence and Lifter Height.

(8) The model accurately predicts the overflow rate of water in a lift-overflow system.

(9) The model shows that the important parameter is the volumetric flow rate of gas and not the molar flow rate of gas. Consequently, the application of vacuum to a system enhances lift and overflow rates for a given molar gas flow rate.

(10) Although future work should be done on liquid metals, the model is thought to be applicable to gas injection into liquid metals.

REFERENCES

(1) Wallis, G.B.: One Dimensional Two Phase Flow, McGraw Hill Book Co.,New York, NY, 1969.

(2) Martinelli, R.C., L.M.K. Boeter, and T.H.M. Taylor: Isothermal Pressure Drop for Two-Phase Two-Component Flow in a Horizontal Pipe, Trans ASME, Feb 1944, Vol. 66, pp. 139-151.

(3) Martinelli, R.C., and D.B. Nelson: Prediction of Pressure Drop During Forced Circulation Boiling of Water, Trans ASME, Aug. 1948, Vol.70, pp.695-702.

(4) Lockhart, R.W., and R.C. Martinelli: Proposed Correlation of Data for Isothermal Two-Phase Two-Component Flow in Pipes, Chem. Eng. Prog., Jan. 1949, Vol.45, pp.39-48.

(5) Zuber, N., and J.A. Findlay: Average Volumetric Concentration in Two-Phase Flow Systems, Trans. ASME, Nov. 1965, pp. 453-468.

(6) Smissaert, G.E.: Two-Component,Two-Phase Flow Parameters for Low Circulation Rates, Argonne National Laboratory, Report 6755, July 1963.

(7) Leibson, I., E.G. Holcomb, A. Gacoso, and J. Jacmic: Rate of Flow And Mechanics of Bubble Formation From Single Submerged Orifices, A.I.Ch.E. Journal, Sept. 1956, pp. 296-306.

(8) Peebles, F.N., and H.J. Garber: Studies on the Motion of Gas Bubbles in Liquids, Chem. Eng. Progress, Vol. 49, Feb. 1953, pp. 88-97.

(9) White,E.T., and R.H. Beardmore: The Velocity of Rise of Single Cylindrical Air Bubbles Through Liquids Contained in Vertical Tubes, Chem. Eng. Science, Vol. 17, 1962, pp. 351-361.

(10) Moissis,R., and P. Griffith: Entrance Effects in a Two-Phase Slug Flow, Journal of Heat Transfer, Trans. ASME, Vol. 84, 1962, pp. 29-39.

(11) Nicklin, D.J., J.O. Wilkes, and J.F. Davidson: Two-Phase Flow in Vertical Tubes, Trans. I. Ch. E., Vol. 40, 1962, pp. 61-68.

(12) Zuber, N., and J. Hench: Steady State and Transient Void Fraction of Bubbling Systems and Their Operating Limits, Nuclear Science and Engineering, 1966.

(13) Harmathy, T.: Velocity of Large Drops and Bubbles in Media of Infinite and of Restricted Extent, A.I.Ch.E. Journal, Vol. 6, 1960, pp. 281-

(14) Szekely, J., and N.J. Themelis: Rate Phenomena in Process Metallurgy, John Wiley and Sons, New-York, NY, 1971.

(15) Narita, K., Y. Satoh, T. Mori, T. Ito, and A. Kujime: On the Circulation Flow Rate and the Desulphurization of Molten Pig Iron in Gas-Lift Mixing Reactor Process, Trans. ISIJ, Vol. 16, 1976, pp. 504-512.

(16) Harris, R.: Gas Injection Enhanced Vacuum Refining of Liquid Metals, Scanninject III, 2nd Intl. Conf. on Injection Metallurgy, MEFOS, Lulea, Sweden, 1983, pp.P1-P10.

(17) Harris, R., and W.G. Davenport: Vacuum Distillation of Liquid Metals Theory and Experimental Study, Met.Trans. B, Vol. 13B, Dec. 1982, pp. 581-588.

(18) Harris, R., and W.G. Davenport: Vacuum Distillation of Liquid Metals Photographic study, Met. Trans. B, Vol. 13B, Dec. 1982, pp. 589-591.

(19) Miller, R.W.: Flow Measurement Engineering Handbook, McGraw Hill Book Company, New-York, NY, 1983.

(20) CRC Handbook of Chemistry and Physics, 64th Edition, CRC Press Inc., Boca Raton, Florida, 1983-1984, pp. F20-F50.

APPENDIX I

```
/LOAD WATFIV
C
C          THIS PROGRAM CALCULATES THE OVERFLOW RATE
C                  IN A GAS-LIFT PUMP.
C
C          THE VALUES OF THE DISTRIBUTION PARAMETER
C               AND THE TERMINAL VELOCITY HAVE
C                    TO BE ENTERED FIRST.
C
C
10     WRITE(6,1000)
       WRITE(6,1001)
       READ(9,*)ASLOPE,V1NF
C
C          IF DESIRED, THE PROGRAM IS   ABLE TO VARY
C          CONTINUOUSLY ONE PARAMETER ( FLOW RATE ,
C          NOZZLE SUBMERGENCE , DIAMETER OF LIFTER,
C          OR LENGTH OF LIFTER ABOVE THE LIQUID ).
C
       WRITE(6,1500)
       WRITE(6,1501)
       WRITE(6,1502)
       WRITE(6,1503)
       WRITE(6,1504)
       WRITE(6,1510)
       READ(9,*)XN
       IF (XN.EQ.0.0)  GOTO 70
       GOTO 80
C
C          HERE , ALL PARAMETERS HAVE TO BE DEFINED.
C
70     WRITE(6,2000)
       WRITE(6,2001)
       WRITE(6,2002)
       WRITE(6,2003)
       READ(9,*)D,FRPTOP,XNS,H
       XY=FRPTOP
       GOTO 100
C
C        THE MINIMUM AND MAXIMUM VALUES OF THE VARIABLE
C                    HAVE TO BE SPECIFIED.
C
80     WRITE(6,1600)
       WRITE(6,1601)
       READ(9,*)XMIN,XMAX
       XINC=(XMAX-XMIN)/50.0
       IF (XN.EQ.1.0) GOTO 95
       IF (XN.EQ.2.0) GOTO 92
       IF (XN.EQ.3.0) GOTO 89
```

```
C
C        THE LENGTH OF LIFTER ABOVE THE IDLE LIQUID
C        SURFACE IS VARYING BETWEEN THE TWO SPECIFIED
C        LIMITS.OTHER PARAMETERS HAVE TO BE ENTERED.
C
      WRITE(6,2000)
      WRITE(6,2001)
      WRITE(6,2002)
      READ(9,*)D,FRPTOP,XNS
      XY=FRPTOP
      WRITE(6,1005)
      WRITE(6,1004)
      WRITE(6,1002)
      WRITE(6,1004)
      WRITE(6,1005)
      DO 87 J=1,51
      H=XMIN+(J-1)*XINC
      CALL CALC(ASLOPE,VINF,D,FRPTOP,XNS,H,XY)
 87   CONTINUE
      GOTO 3000
C
C        THE NOZZLE SUBMERGENCE IS VARYING BETWEEN
C        THE TWO SPECIFIED LIMITS, OTHER PARAMETERS
C        HAVE TO BE ENTERED.
C
 89   WRITE(6,2000)
      WRITE(6,2001)
      WRITE(6,2003)
      READ(9,*)D,FRPTOP,H
      XY=FRPTOP
      WRITE(6,1005)
      WRITE(6,1004)
      WRITE(6,1002)
      WRITE(6,1004)
      WRITE(6,1005)
      DO 90 J=1,51
      XNS=XMIN+(J-1)*XINC
      CALL CALC(ASLOPE,VINF,D,FRPTOP,XNS,H,XY)
 90   CONTINUE
      GOTO 3000
C
C        THE FLOW RATE IS VARYING BETWEEN THE TWO
C        SPECIFIED LIMITS, OTHER PARAMETERS HAVE
C        TO BE DEFINED.
```

```
C
92    WRITE(6,2000)
      WRITE(6,2002)
      WRITE(6,2003)
      READ(9,*)D,XNS,H
      XY=XMIN
      WRITE(6,1005)
      WRITE(6,1004)
      WRITE(6,1002)
      WRITE(6,1004)
      WRITE(6,1005)
      DO 93 J=1,51
      FRPTOP=XMIN+(J-1)*XINC
      CALL CALC(ASLOPE,VINF,D,FRPTOP,XNS,H,XY)
93    CONTINUE
      GOTO 3000
C
C        THE DIAMETER OF THE LIFTER IS VARYING
C        BETWEEN THE TWO SPECIFIED LIMITS, OTHER
C        PARAMETERS HAVE TO BE DEFINED.
C
95    WRITE(6,1999)
      WRITE(6,2001)
      WRITE(6,2002)
      WRITE(6,2003)
      READ(9,*)FRPTOP,XNS,H
      XY=FRPTOP
      WRITE(6,1005)
      WRITE(6,1004)
      WRITE(6,1002)
      WRITE(6,1004)
      WRITE(6,1005)
      DO 96 J=1,51
      D=XMIN+(J-1)*XINC
      CALL CALC(ASLOPE,VINF,D,FRPTOP,XNS,H,XY)
96    CONTINUE
      GOTO 3000
100   WRITE(6,1005)
      WRITE(6,1004)
      WRITE(6,1002)
      WRITE(6,1004)
      WRITE(6,1005)
      CALL CALC(ASLOPE,VINF,D,FRPTOP,XNS,H,XY)
C
C
1000  FORMAT(5X,'ENTER IN A FREE FORMAT "CO" (SUGGESTED 1.71)')
1001  FORMAT(5X,'AND TERMINAL VELOCITY (SUGGESTED 28.0)')
1002  FORMAT(10X,'*  D  * FLOW RATE  *     H     *     NS     *    OUTL
     &   *')
1004  FORMAT(10X,'*     *             *           *            *
     &   *')
```

```
1005  FORMAT(10X,'**********************************************
     1****')
1500  FORMAT(5X,'IF YOU WANT TO VARY ONE PARAMETER (D,FR,HS OR H),
1501  FORMAT(5X,'TYPE 1 TO VARY THE DIAMETER')
1502  FORMAT(5X,'TYPE 2 TO VARY THE FLOW RATE')
1503  FORMAT(5X,'TYPE 3 TO VARY THE NOZZLE SUBMERGENCE')
1504  FORMAT(5X,'TYPE 4 TO VARY THE LIFT')
1510  FORMAT(5X,'OTHERWISE TYPE 0.')
1600  FORMAT(5X,'ENTER IN A FREE FORMAT THE MINIMUM AND MAXIMUM VALUES
1601  FORMAT(5X,'OF YOUR VARIABLE,THERE WILL BE 50 POINTS CALCULATED
1999  FORMAT(5X,'ENTER IN A FREE FORMAT')
2000  FORMAT(5X,'ENTER IN A FREE FORMAT DIAMETER OF LITTER (CM),')
2001  FORMAT(5X,'FLOW RATE (TOP PRESS.,PSI)')
2002  FORMAT(5X,'NOZZLE SUBMERGENCE (CM),')
2003  FORMAT(5X,'AND LENGTH OF TUBE ABOVE SURFACE (CM),')
C
C        IT IS POSSIBLE TO DO MORE COMPUTATION
C
7000  WRITE(6,1005)
      WRITE(6,3001)
      READ(5,*)XX
      IF(XX.EQ.0.0)GOTO 4000
      GOTO 10
3001  FORMAT('TYPE 1  IF YOU WISH TO DO MORE COMPUTATIONS,0 OTHERWISE')
4000  STOP
      END
C
C
C        SUBROUTINE SOLVING THE FIFTH DEGREE EQUATION
C        WHICH GIVES THE VALUE OF THE OVERFLOW, USING
C        THE SECANT'S METHOD.NEGATIVE VALUES ARE NOT
C        TAKEN INTO ACCOUNT.
C
C
      SUBROUTINE CALC(ASLOPE,VINF,D,FRPTOP,XNS,H,XY)
      G=981.0
      PI=ARCOS(-1.0)
      A=PI*D**2/4.0
      HCOMP=XNS*FRPTOP
      HCOMP=HCOMP/((ASLOPE-1)*FRPTOP+VINF*A)
      XA=XNS*FRPTOP*((H/HCOMP)-1)
      XB=ASLOPE*H
      XC=(ASLOPE-1.0)*FRPTOP+VINF*A
      XD=XC+FRPTOP
      XE=ASLOPE
      X6=XE**3
      X5=3.0*XD*XE**2
      X4=3.0*(XD**2)*XE+G*(A**2)*XB*XE**2
      X3=XD**3+2*G*(A**2)*XC*XE*XB+G*XA*(A*XE)**2
      X2=G*XB*(A*XC)**2+2*G*XC*XE*XA*A**2
      X1=G*XA*(A*XC)**2
```

```
      ERR=1.0E-1
       Y1=XY
       Y2=XY+10000.0
25     Y3=X6*Y1**5+X5*Y1**4+X4*Y1**3+X3*Y1**2+X2*Y1+X1
       Y4=X6*Y2**5+X5*Y2**4+X4*Y2**3+X3*Y2**2+X2*Y2+X1
       XY=(Y1*Y4-Y2*Y3)/(Y4-Y3)
       Y1=Y2
       Y2=XY
       EPS=ABS(Y2-Y1)
       IF(EPS.LE.ERR) GOTO 29
       GOTO25
29     IF(Y2.GE.0.0) GOTO 30
       Y2=0.0
30     WRITE(6,1004)
       WRITE(6,1003)D,CRPTOP,H,XNS,Y2
       WRITE(6,1004)
1003   FORMAT(10X,'*',F5.1,'*  ',F9.1,'   * ',F7.2,'   * ',F7.2,'     *
      $F9.1,'  *')
1004   FORMAT(10X,'*      *            *            *            *
      $    *')
       RETURN
       END
/ENDRUN
```

THIS IS A TYPICAL OUTPUT OBTAINED WITH THIS PROGRAM.

```
   ENTER IN A FREE FORMAT "CO" (SUGGESTED 1.71)
   AND TERMINAL VELOCITY (SUGGESTED 28.0)
?
1.71 28
   IF YOU WANT TO VARY ONE PARAMETER (D,FR,NS OR H),
   TYPE 1 TO VARY THE DIAMETER
   TYPE 2 TO VARY THE FLOW RATE
   TYPE 3 TO VARY THE NOZZLE SUBMERGENCE
   TYPE 4 TO VARY THE LIFT
   OTHERWISE TYPE 0.
?
0

   ENTER IN A FREE FORMAT DIAMETER OF LIFTER (CM),
   FLOW RATE (TOP PRESS.,CC/S) ,
   NOZZLE SUBMERGENCE (CM),
   AND LENGTH OF TUBE ABOVE SURFACE (CM).
?
30 200000 220 20
      ***************************************************
      *    *            *          *          *         *
      *  D * FLOW RATE  *     H    *     NS   *    OVFL   *
      *    *            *          *          *         *
      ***************************************************
      *    *            *          *          *         *
      * 30.0*  200000.0  *   20.00  *  220.00  *   115392.3 *
      *    *            *          *          *         *
      ***************************************************
TYPE 1 IF YOU WISH TO DO MORE COMPUTATIONS,0 OTHERWISE
?
0
```